AD-A084 941 ARMY ELECTRONICS RESEARCH AND DEVELOPMENT COMMAND WS--ETC F/G 17/5
RELATIONSHIPS BETWEEN RADIATIVE PROPERTIES AND MASS CONTENT OF --ETC(U)
APR 80 R G PINNICK, S G JENNINGS
UNCLASSIFIED ERADCOM/ASL-TR-0052 NL

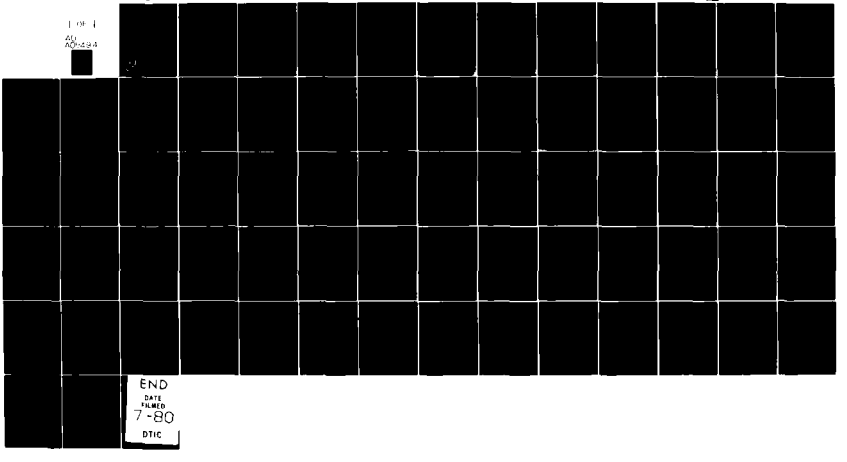

END
DATE FILMED
7-80
DTIC

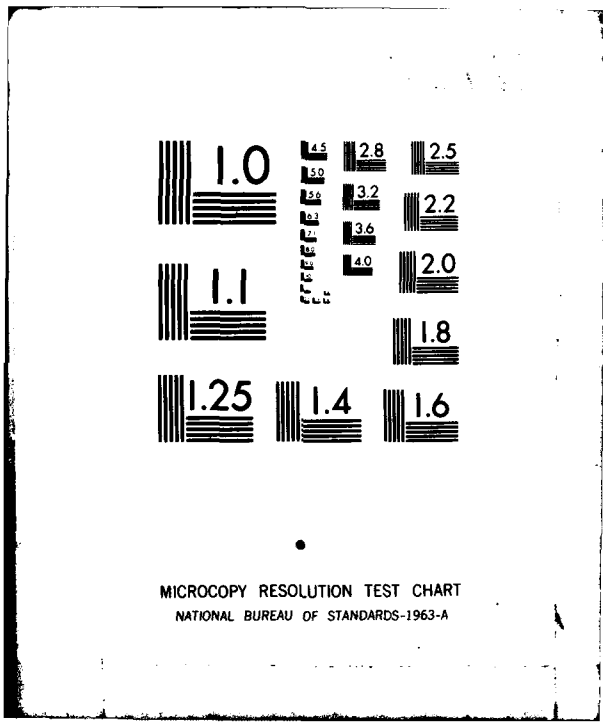
1.0
1.1
1.25
1.4
1.6
1.8
2.0
2.2
2.5
2.8
3.2
3.6
4.0
4.5
5.0
5.6
6.3
MICROCOPY RESOLUTION TEST CHART
NATIONAL BUREAU OF STANDARDS-1963-A

ASL-TR-0052

LEVEL II

AD

Reports Control Symbol
OSD-1366

AD A084941

RELATIONSHIPS BETWEEN RADIATIVE PROPERTIES AND MASS CONTENT OF PHOSPHORIC ACID, HC, PETROLEUM OIL, AND SULFURIC ACID MILITARY SMOKES

DTIC ELECTE JUN 2 1980 C

APRIL 1980

By

R.G. PINNICK

US ARMY ATMOSPHERIC SCIENCES LABORATORY
White Sands Missile Range, New Mexico 88002

S.G. JENNINGS

DEPARTMENT OF PURE AND APPLIED PHYSICS
University of Manchester Institute of Science and Technology
Manchester, England

US Army Electronics Research and Development Command
ATMOSPHERIC SCIENCES LABORATORY
White Sands Missile Range, NM 88002

NOTICES

Disclaimers

The findings in this report are not to be construed as an official Department of the Army position, unless so designated by other authorized documents.

The citation of trade names and names of manufacturers in this report is not to be construed as official Government indorsement or approval of commercial products or services referenced herein.

Disposition

Destroy this report when it is no longer needed. Do not return it to the originator.

SECURITY CLASSIFICATION OF THIS PAGE *(When Data Entered)*

REPORT DOCUMENTATION PAGE

READ INSTRUCTIONS BEFORE COMPLETING FORM

1. REPORT NUMBER: ERADCOM/ASL-TR-0052	2. GOVT ACCESSION NO.
3. RECIPIENT'S CATALOG NUMBER	
4. TITLE *(and Subtitle)*: RELATIONSHIPS BETWEEN RADIATIVE PROPERTIES AND MASS CONTENT OF PHOSPHORIC ACID, HC, PETROLEUM OIL, AND SULFURIC ACID MILITARY SMOKES.	5. TYPE OF REPORT & PERIOD COVERED: Technical Report.
	6. PERFORMING ORG. REPORT NUMBER
7. AUTHOR(s): R. G. Pinnick, S. G. Jennings	8. CONTRACT OR GRANT NUMBER(s)
9. PERFORMING ORGANIZATION NAME AND ADDRESS: Atmospheric Sciences Laboratory, White Sands Missile Range, New Mexico 88002	10. PROGRAM ELEMENT, PROJECT, TASK AREA & WORK UNIT NUMBERS: DA Task No. 1L161102B53A 13
11. CONTROLLING OFFICE NAME AND ADDRESS: US Army Electronics Research and Development Command, Adelphi, MD 20783	12. REPORT DATE: April 1980
	13. NUMBER OF PAGES: 70
14. MONITORING AGENCY NAME & ADDRESS *(if different from Controlling Office)*	15. SECURITY CLASS. *(of this report)*: UNCLASSIFIED
	15a. DECLASSIFICATION/DOWNGRADING SCHEDULE

16. DISTRIBUTION STATEMENT *(of this Report)*

Approved for public release; distribution unlimited.

17. DISTRIBUTION STATEMENT *(of the abstract entered in Block 20, if different from Report)*

18. SUPPLEMENTARY NOTES

19. KEY WORDS *(Continue on reverse side if necessary and identify by block number)*

Smoke obscuration
Smoke extinction coefficients
Extinction-mass relationships for smoke
Infrared extinction in smoke
Backscatter-extinction relationships in smoke
Single scatter albedos in smoke

20. ABSTRACT *(Continue on reverse side if necessary and identify by block number)*

The tactical effectiveness of military electro-optical devices such as the forward looking infrared or high energy laser (HEL) systems requires a knowledge of the extinction (absorption and scattering) by the intervening atmosphere. In the case of intentionally produced obscurants such as smokes, a quantitative assessment of these effects generally requires knowledge of the size distribution and concentration of the particles. A relation between the radiative properties of smoke particles and their mass content, even if it is an approximate one, would reduce the complexity of this assessment. One would then

DD FORM 1 JAN 73 1473 EDITION OF 1 NOV 65 IS OBSOLETE 1

SECURITY CLASSIFICATION OF THIS PAGE *(When Data Entered)*

410663

20. ABSTRACT (cont)

only need to know the spacial distribution of the mass content of the smoke particles rather than the details of their particle size distributions and number concentrations. In this report, a linear relation, independent of particle size distribution, between aerosol volume extinction coefficient and mass content is derived and applied to several military smokes: solutions of orthophosphoric acid in water, zinc chloride in water (HC smoke), diesel fuel, fog oil, and sulfuric acid smoke. Comparison of the theoretical extinction-mass relation with infrared (IR) transmission measurements of Milham (1976), Milham et al (1977), and Carlon et al (1977) shows good agreement (generally within 30 percent) between theory and measurement for the highly absorbing phosphoric acid and sulfuric acid smokes, but only fair-to-poor agreement (up to factors of 2.5 to 10 differences) for weakly absorbing HC and fog oil smokes. Relationships between smoke aerosol volume absorption coefficient and aerosol mass and between aerosol volume backscatter coefficient and mass are also derived. The relationships are valid only at particular wavelengths that depend on the aerosol refractive index and on the range of particle sizes present in a particular polydispersion. Several applications are suggested: (1) prediction of IR (and in some cases visible) extinction coefficient from knowledge of smoke cloud mass content; or, conversely (2) inference of path-integrated smoke mass content from an IR laser transmission measurement through the smoke cloud; (3) determination of smoke mass content at a particular point in a smoke cloud from a smoke aerosol absorption measurement with an IR laser spectrophone; (4) determination of smoke backscatter coefficient from knowledge of smoke mass content; (5) inference of extinction at one IR wavelength from knowledge of that at another IR wavelength; and (6) prediction of phosphoric acid and HC smoke extinction coefficient as a function of atmospheric relative humidity from knowledge of smoke mass expenditure.

PREFACE

We gratefully acknowledge M. E. Milham for supplying the refractive indexes of the orthophosphoric acid and zinc chloride solutions and Gottfried Hänel for the particle size-humidity predictions for these solutions.

CONTENTS

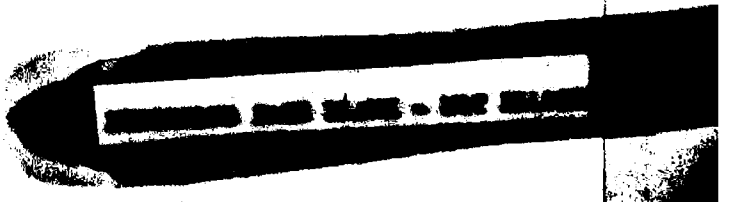

INTRODUCTION

During the last decade, a number of scientists[1-4] have investigated possible relationships between extinction (or atmospheric visibility) and mass content of atmospheric aerosols. In general, these investigations indicate that there is no unique relation between extinction and aerosol mass although an approximate proportionality may exist for specific locations or aerosol type.

However, smoke particles are distinctly different from natural aerosol particles in three respects: they are generally smaller, more nearly homogeneous, and generally spherical in shape. These three properties enable us to derive a unique relation, independent of the particle size distribution, between the IR (and in some cases visible) extinction coefficient and mass concentration for phosphoric acid, HC, petroleum oil, and sulfuric acid smokes. These extinction-mass relationships are extended to relations between aerosol absorption coefficient and mass content, and between aerosol backscatter coefficient and mass content.

Our results have considerable practical application. They suggest that knowledge of smoke mass content implies knowledge of IR (and in some cases visible) extinction coefficient. Alternatively, smoke mass content could be inferred from IR transmission measurements, IR spectrophone absorption measurements, or visible-wavelength lidar backscatter measurements.

EXTINCTION, ABSORPTION, BACKSCATTER, AND MASS CONTENT OF SMOKES

Consider a polydispersion of spherical smoke particles characterized by a size distribution n(r). We want to derive relationships between the aerosol extinction and absorption coefficients σ_e and σ_a, the backscatter coefficient σ_{bs}, and the aerosol mass content M given by

---

[1]R. J. Charlson, N. C. Ahlquist, and H. Horvath, 1968, On the Generality of Correlation of Atmospheric Mass Concentration and Light Scatter, Atmos Environ, 2:455-464

[2]K. E. Noll, P. K. Mueller, and M. Imada, 1968, Visibility and Aerosol Concentration in Urban Air, Atmos Environ, 2:465-475

[3]M. J. Pilat and D. S. Ensor, 1970, Plume Opacity and Particulate Mass Concentration, Atmos Environ, 4:163-173

[4]E. M. Patterson and D. A. Gillette, 1977, Measurements of Visibility vs Mass-Concentration for Airborne Soil Particles, Atmos Environ, 11:193-196

$$\sigma_e = \int \pi r^2 Q_e(m,x) n(r) dr \ , \tag{1}$$

$$\sigma_a = \int \pi r^2 Q_a(m,x) n(r) dr \ , \tag{2}$$

$$\sigma_{bs} = \frac{1}{4\pi} \int \pi r^2 G(m,x) n(r) dr \ , \tag{3}$$

$$M = \rho \int \frac{4}{3} \pi r^3 n(r) dr \ , \tag{4}$$

where ρ is the smoke aerosol density, Q_e (m,x) and Q_a (m,x) are the efficiency factors for extinction and absorption for a particle with refractive index m and size parameter $x = 2\pi r/\lambda$, and G (m,x) is the backscatter efficiency (or gain) defined as the ratio of the backscatter cross section to the geometric area. These efficiency factors multiplied by πr^2 give the corresponding single-particle cross sections. In general the extinction, absorption, and backscatter efficiencies are rather complicated functions of particle size, refractive index, and wavelength.

Examples of the behavior of the efficiency factors for extinction (for 38 percent sulfuric acid in water at wavelengths λ = 0.55μm, 9.5μm), absorption (for 38 percent sulfuric acid at λ = 10.6μm), and backscattering (for 75 percent sulfuric acid at λ = 0.694μm) are shown in figures 1 through 4. Numerous other examples for other smokes and other wavelengths are given in the appendix, figures A-1 through A-10.

For particles large compared to the wavelength ($x >> 1$), $Q_e \to 2$ and $Q_a \to 1 - \left|\frac{m-1}{m+1}\right|^2$ as shown by Chýlek;[5] for small particles ($x << 1$), more complicated expressions can be worked out for Q_e and Q_a (Penndorf).[6] For particles having sizes outside the large particle asymptotic region and the Rayleigh region, the rigorous Mie theory must

---

[5]Petr Chýlek, 1975, Asymptotic Limits of the Mie-Scattering Characteristics, J Opt Soc Amer, 65:1316-1318

[6]R. B. Penndorf, 1962, Scattering and Extinction Coefficients for Small Spherical Aerosols, J Atmos Sci, 19:193

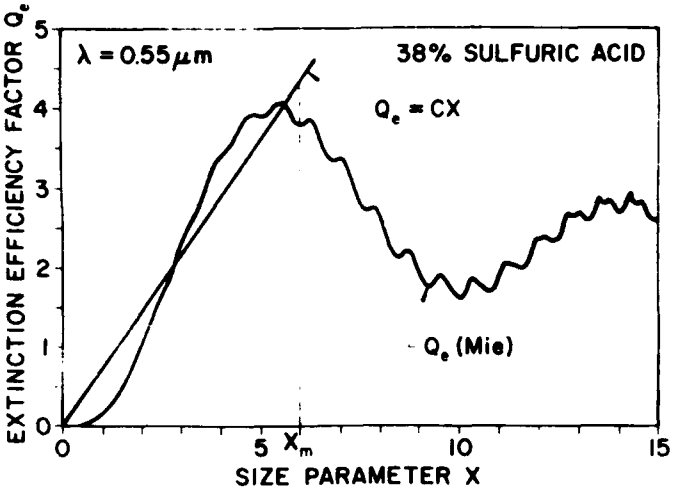

Figure 1. Efficiency factor for extinction Q_e for 38 percent sulfuric acid (62 percent water) droplets at a wavelength $\lambda = 0.55\mu m$ (index of refraction $m = 1.394-0i$) and its approximation by a straight line $Q_e(x) = cx$ for $x \leq x_m$. The approximation overestimates the exact value of Q_e at small size parameters x, and underestimates it at larger x (still with $x \leq x_m$). These two errors tend to cancel out in the evaluation of the integral in equation (1).

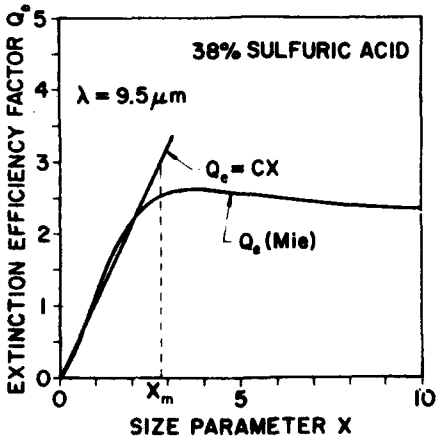

Figure 2. As in figure 1 except for $\lambda = 9.5\mu m$. Due to the large imaginary index at this wavelength ($m = 1.46-0.38i$) the character of the $Q_e(x)$ curve differs markedly from that at $\lambda = 0.55\mu m$. The $Q_e(x)$ curve again lends itself to approximation by a straight line $Q_e(x) = cx$ for $x < x_m$, in this case more accurately than the $Q_e(x)$ curve in figure 1. As in figure 1, the approximation overestimates the exact value of Q_e for some size parameters x, but underestimates it for others (with $x < x_m$) leading to cancellation of these errors in the evaluation of the integral in equation 1. However, since the approximation is so good for all size parameters $x < x_m$ it is not necessary for particles of a polydispersion to have size parameters x throughout the range $o < x < x_m$ for the linear relation (5) to be fairly accurate, as cancellation of errors is not so important (as it is at $\lambda = 0.55\mu m$).

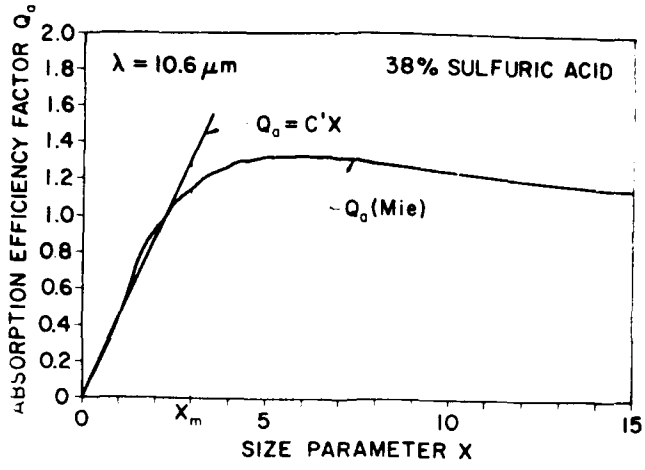

Figure 3. As in figure 2 except for the efficiency factor for absorption at $\lambda = 10.6\mu m$ (refractive index of 38 percent sulfuric acid at this wavelength is taken to be $m = 1.48-0.17i$). The $Q_a(x)$ curve can be well approximated by a straight line $Q_a(x) = c'x$ for $x \leq x_m$ leading to the size-distribution-independent linear relation between aerosol absorption coefficient and mass content according to equation (6).

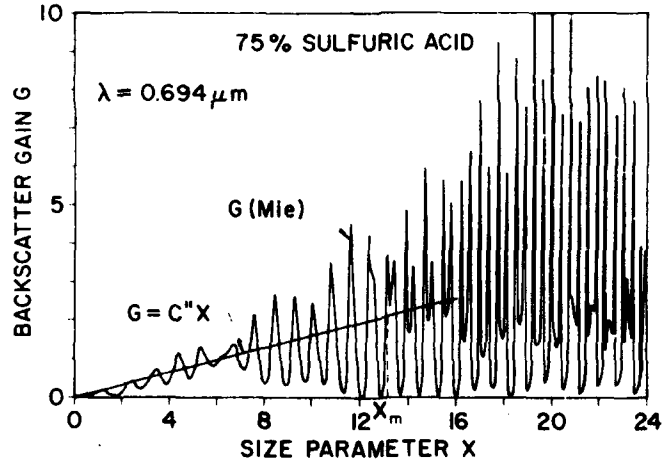

Figure 4. Normalized backscatter gain G for 75 percent sulfuric acid droplets at the ruby laser wavelength $\lambda = 0.694\mu m$ ($m = 1.428-2 \times 10^{-8}i$) and its approximation by a straight line $G(x) = c"x$ for $x < x_m$. The approximation overestimates the exact value of g at some size parameters x, but underestimates it at others (still with $x < x_m$). These two errors tend to cancel out in the evaluation of the integral in equation (3). For backscatter this cancellation of error is particularly important (as compared to extinction and absorption in figures 1 through 3) because for some size parmeters (for example $x = 8$) the value of $G = c" x$ differs considerably from the exact value. However, we do not necessarily have to have particles with radii throughout the entire range $o < x < x_m$ for cancellation of errors to occur.

generally be used. However, we propose to approximate the efficiency factors $Q_e(x)$, $Q_a(x)$, and $G(x)$ for particles having radii less than some maximum value r_m (where $r_m = x_m\lambda/2\pi$) by linear functions of particle size parameter $Q_e = cx$, $Q_a = c'x$, and $G = c''x$ as shown in figures 1 through 4 and A-1 through A-10. The parameters c, c', and c'' are then functions only of particle refractive index which is, in turn, a function of material composition and wavelength. This approximation procedure was originally used by Chýlek[7] for atmospheric cloud and fog droplets. The consequence of utilizing these simple linear approximations for the Mie efficiency factors in the expressions for aerosol extinction, absorption, and backscatter coefficients given by equations (1) through (3) are far reaching. This is because these expressions now contain the integral $\int r^3 n(r)dr$, and thus the coefficients become proportional to aerosol mass and independent of the particle size distribution n(r):

$$\sigma_e = \frac{3\pi c}{2\lambda\rho} M , \tag{5}$$

$$\sigma_a = \frac{3\pi c'}{2\lambda\rho} M , \tag{6}$$

$$\sigma_{bs} = \frac{3c''}{8\lambda\rho} M , \tag{7}$$

where $c(\lambda)$, $c'(\lambda)$, and $c''(\lambda)$ are the slopes of the straight lines approximating the Mie efficiency factors as in figures 1 through 4 and A-1 through A-10. If the refractive index $m(\lambda)$ is a slowly varying function of wavelength, then we might expect $c(\lambda)$, $c'(\lambda)$, and $c''(\lambda)$ to be slowly varying functions of wavelength leading to the extinction, absorption, and backscatter coefficients σ_e, σ_a, and σ_{bs} being proportional to $1/\lambda$.[8,9]

[7]Petr Chýlek, 1978, Extinction and Liquid Water Content of Fogs and Clouds, J Atmos Sci, 35:296-300

[8]R. G. Pinnick, D. L. Hoihjelle, G. Fernandez, E. B. Stenmark, J. D. Lindberg, S. G. Jennings, and G. B. Hoidale, 1978, Vertical Structure in Atmospheric Fog and Haze and Its Effects on IR and Visible Extinction, J Atmos Sci, 35:2020-2032

[9]Petr Chýlek, J. T. Kiehl, and M. K. W. Ko, 1979, Infrared Extinction and the Mass Concentration of Atmospheric Aerosols, Atmos Environ, 13:169-173

The equation (5) relating aerosol extinction coefficient and mass content is distinctly different from that of Box and McKellar[10] who derived a relation between spectrally integrated aerosol optical depth and columnar mass content. The primary distinction is that Box and McKellar's result is integrated over all wavelengths, whereas our expression (5) holds at a particular wavelength. Also, Box and McKellar do not approximate the extinction efficiency factor by a linear function of size parameter.

It might be argued that in some cases approximating the extinction efficiency factor Q_e (figure 1) and the backscatter gain G (figure 4) with linear functions of particle size parameter might be rather precarious. However, note in these cases that for some values of $x < x_m$ the $Q_e = cx$ (or $G = c''x$) approximation overestimates the exact Mie result, while for other values of $x < x_m$ the opposite is true. These approximations are more accurate if size distributions of particles have a range of size parameters throughout much of the regime $o < x < x_m$ so that cancellation of errors in evaluation of the integrals in equations (1) and (3) can occur. Chance of cancellation is particularly important in backscattering, where differences between the approximation and the exact Mie result are sometimes large.

Keeping in mind the cancellation-of-error factor, we have carried out the procedure of approximating the extinction, absorption, and backscatter efficiency factors for phosphoric acid, HC, diesel oil, fog oil, and FS smokes at selected visible and IR wavelengths. Concentrations of 20, 50, 65, and 85 percent orthophosphoric acid in water; 20, 65, 50, 40, and 75 percent zinc chloride in water (HC smoke); and 38, 75 percent sulfuric acid in water (FS smoke) were used in the calculations. The indexes of refraction for the orthophosphoric acid and zinc chloride solutions were measured by Querry and Tyler[11] and provided by M. E. Milham of the Chemical Systems Laboratory.* The index values for fuel and petroleum oils were taken from Conner and Hodkinson[12] and Hale et al;[13] those for the sulfuric acid solutions were taken from Palmer and Williams.[14]

[10]M. A. Box and B. H. J. McKellar, 1978, Direct Evaluation of Aerosol Mass Loadings from Multispectral Extinction Data, Quart J Roy Meteorol Soc, 104:755-781

[11]M. R. Querry and I. L. Tyler, 1978, Complex Refractive Indices in the Infrared for H_3PO_4 in Water, J Opt Soc Am, 68:1404

*Private communication, 1978

[12]W. D. Conner and J. R. Hodkinson, 1967, Optical Properties and Visual Effects of Smoke-Stack Plumes, US Department of Health, Education, and Welfare, Public Health Service Publication, 999-AP-30

[13]G. M. Hale, I. L. Tyler, and M. R. Querry, 1978, Complex Refractive Indices in the Infrared for Selected Oils and Alcohols, J Opt Soc Am, 68:1403

[14]K. F. Palmer and D. Williams, 1975, Optical Constants of Sulfuric Acid: Application to the Clouds of Venus? Appl Opt, 14:208-219

The results for aerosol extinction and absorption are summarized in tables A-1 through A-13 in the appendix. Given for various wavelengths are values of the slope parameter c (or c′) of a straight line approximating the efficiency factor $Q_e(m,x)$ (or $Q_a[m,x]$) for $x \leq x_m$ (or equivalently for $r \leq r_m$); values of the quantity $3\pi c/2\lambda\rho$ (or $3\pi c'/2\lambda\rho$) which if multiplied by the smoke mass content give the extinction (or absorption) coefficient according to equations (5) and (6); and values of the ratio of absorption to extinction coefficients σ_a/σ_e. Estimates of maximum errors in the values of $3\pi c/2\lambda\rho$ (or $3\pi c'/2\lambda\rho$) resulting from errors in the $Q_e = cx$ (or $Q_a = c'x$) approximation are also shown in the tables. No values are shown when the estimated errors exceed 100 percent. The reader should be cautioned that the values of the ratio of absorption to extinction coefficients σ_a/σ_e can be used only if the maximum radius conditions are satisfied for both extinction and absorption.

Some obvious conclusions drawn from tables A-1 through A-13 are as follows:

a. For phosphoric acid solutions in water (tables A-1 through A-4), the slope parameter $c(\lambda)$ is a slowly varying function of wavelength for $3\,\mu m \leq \lambda \leq 5\,\mu m$. This implies that the extinction coefficient should have $1/\lambda$ wavelength dependence in this spectral region according to equation (5). The same conclusion applies to the HC smoke solutions (tables A-5 through A-9) where the slope parameter $c(\lambda)$ is even less sensitive to wavelength in the 3μm to 4μm region. For the longer 8μm to 12μm wavelength range the slope parameter $c(\lambda)$ varies by up to a factor 3.4 for phosphoric acid solutions, while in the case of HC smoke the variation is markedly less (at most 50 percent).

b. Phosphoric acid solutions generally have a much lower single scattering albedo than HC smoke solutions. For example, in the 3.5μm to 4μm region the percentage of scattering to extinction is at least 90 percent for HC solutions as compared to 50 to 90 percent for phosphoric acid solutions.

c. For petroleum oil smokes (tables A-10 and A-11) the variation of $c(\lambda)$ throughout the IR is small (about 30 percent), indicating an approximate $1/\lambda$ dependence of extinction coefficient; this is also the case for absorption in the 8μm to 12μm wavelength range. There is, however, considerable fluctuation in $c'(\lambda)$ (up to a factor of about 5) for petroleum smokes in the 3μm to 5μm region.

d. For FS smoke of given mass, 38 percent acid is more effective in causing extinction in the wavelength range $3\,\mu m \leq \lambda \leq 5\,\mu m$ than is 75 percent acid, as can be seen by comparing values of $3\pi c/2\lambda\rho$ in tables A-12 and A-13. The opposite is true for $8\,\mu m \leq \lambda \leq 12\,\mu m$.

A summary of the $G = c''x$ approximation results relating smoke backscatter coefficient to smoke mass content is presented in table A-14. Shown for the ruby ($\lambda = 0.694\,\mu m$) and neodymium-YAG ($\lambda = 1.06\,\mu m$) laser wavelengths are values of the maximum radius r_m, values of the slope parameter $c''(\lambda)$, and values of the quantity $3c''/8\lambda\rho$ which if multiplied by the smoke mass content give the smoke backscatter coefficient σ_{bs} according to equation (7). Note, however, that consideration of even slightly different complex refractive indexes markedly changes the functional form of the backscatter gain and hence the value of $c''(\lambda)$.

APPLICATION TO PHOSPHORIC ACID, HC, PETROLEUM OIL, AND FS SMOKE

Before we can have confidence in applying the linear relationships (5) through (7) between smoke aerosol extinction, absorption, backscatter, and mass content, we should test their validity with existing measurements that are available. Carlon et al,[15] Milham et al,[16] and Milham[17] have measured the transmission through phosphoric acid, red phosphorus, HC, petroleum oil, and sulfuric acid smokes. Most measurements were made in the 3 μm to 5 μm and 7 μm to 13 μm wavelength ranges, although transmission measurements for petroleum oil smoke and FS were made for λ = 0.36 μm to 2.35 μm. The same transmission cell was used for all of the above work and consisted of a 22 m^3 cylindrical test chamber with a transmission path L of 3.05 m length. A smoke mass content measurement was made simultaneously with the transmission measurement by weighing particles collected onto filters.

The extinction coefficient-mass relation (5) must be compared cautiously to measurements of these quantities. The reason is that since extinction coefficients are derived from transmission measurements, forward scattering corrections[18,19] and multiple scattering corrections should be considered. Forward scattering corrections arise from singly scattered photons that enter the detector along with the unscattered (direct) radiation due to the finite angular aperture of the detector. Similarly, multiple scattering corrections arise from signal contributed by multiple scattered photons. Both these effects cause increased detector signal and hence result in a smaller inferred extinction coefficient if they are not taken into account. We estimate the forward scatter corrections for the experimental setup used by Carlon and Milham to be not more than 3 percent and have neglected them; however, no attempt was made to make quantitative estimates of multiple scatter corrections.

---

[15] H. R. Carlon, D. H. Anderson, M. E. Milham, T. L. Tarnove, R. H. Frickel, and I. Sindoni, Infrared Extinction Spectra of Some Common Liquid Aerosols, Appl Opt, 16:1598-1605

[16] M. E. Milham, D. H. Anderson, R. H. Frickel, and T. L. Tarnove, 1977, New Findings on the Nature of WP/RP Smokes, Technical Report ARCSL-TR-77067, US Army ARADCOM, Chemical Systems Laboratory, Aberdeen Proving Ground, MD

[17] M. E. Milham, 1976, A Catalog of Optical Extinction Data for Various Aerosols/Smokes, Report ED-SP-77002, Edgewood Arsenal, Aberdeen Proving Ground, MD

[18] A. Deepak and M. A. Box, 1978, Forward Scattering Corrections for Optical Extinction Measurements in Aerosol Media. 1: Monodispersions, Appl Opt, 17:2900-2908

[19] A. Deepak and M. A. Box, 1978, Forward Scattering Corrections for Optical Extinction Measurements in Aerosol Media. 2: Polydispersions, Appl Opt, 17:3169-3176

PHOSPHORIC ACID AND RP SMOKE

The extinction coefficient-mass relation (5) for 60 percent phosphoric acid smoke is compared to measurements of Milham et al[16] in figures 5 and 6. The agreement is good in both the 3μm to 5μm and 8μm to 12μm spectral regions, as the relation (5) generally overpredicts the extinction to mass ratio σ_e/M, but by not more than about 30 percent [here the slope parameters $c(\lambda)$ were determined by using refractive indexes for 65 percent phosphoric acid rather than 60 percent acid]. This good agreement is not unexpected as the extinction efficiency factors are well approximated by linear functions of particle size parameter in the 3μm to 5μm and 8μm to 12μm spectral regions (see for example figures A-1 and A-2) and the maximum radius conditions are not strongly violated.

In contrast to the phosphoric acid results, comparison of the relation (5) to Milham's[17] measurements on RP smoke (figure 7) shows relatively poor agreement in the 8μm to 12μm spectral region. The reason for the poor agreement is that the burning of RP/WP smokes apparently results in production of an unknown chemical species[16] whose refractive indexes

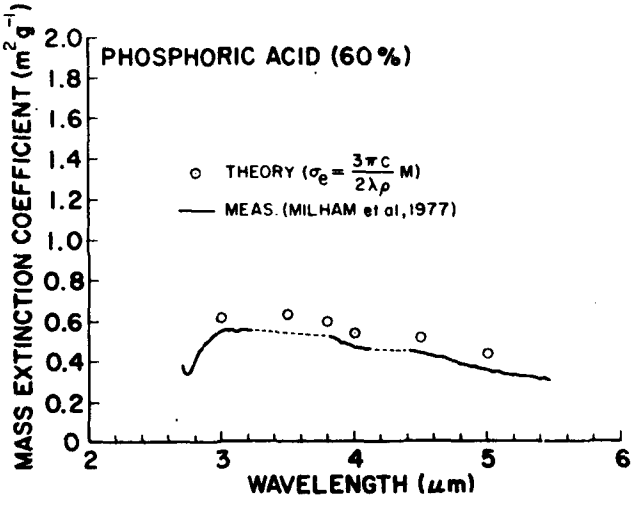

Figure 5. Values of the ratio of aerosol extinction coefficient to mass content predicted according to the linear relation (5) (open circles), and measured by Milham et al (solid line) for 60 percent phosphoric acid aerosol. Since the parameter $c(\lambda)$ is nearly wavelength independent (see table A-3) the relation (5) predicts extinction to have an approximate $1/\lambda$ wavelength dependence in the 3μm to 5μm spectral region.

---

[16] M. E. Milham, D. H. Anderson, R. H. Frickel, and T. L. Tarnove, 1977, New Findings on the Nature of WP/RP Smokes, Technical Report ARCSL-TR-77067, US Army ARADCOM, Chemical Systems Laboratory, Aberdeen Proving Ground, MD

[17] M. E. Milham, 1976, A Catalog of Optical Extinction Data for Various Aerosols/Smokes, Report ED-SP-77002, Edgewood Arsenal, Aberdeen Proving Ground, MD

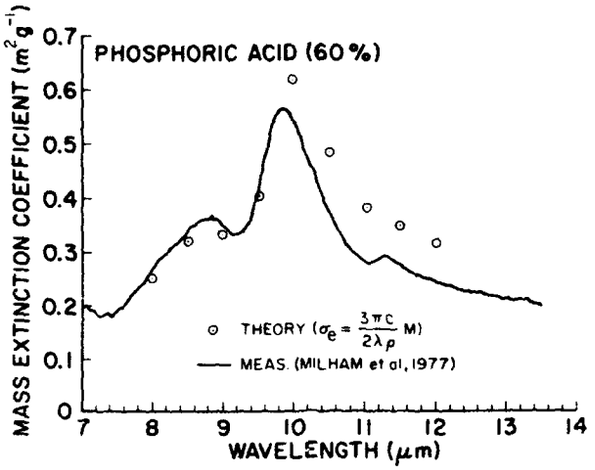

Figure 6. Same as figure 5 except for the 7μm to 14μm spectral region. In this case the parameter c(λ) has considerable spectral character. The agreement between measurement and theory is within 30 percent.

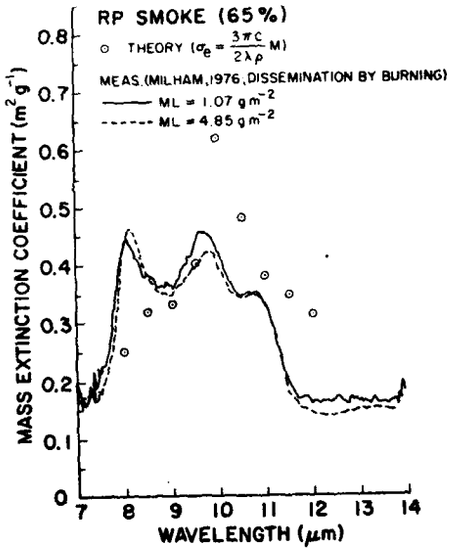

Figure 7. Ratio of aerosol extinction coefficient to mass content predicted according to linear relation (5) (open circles), and measured by Milham (solid and dashed curves) for Red Phosphorus (RP) smoke disseminated by burning. The two measurement curves are for different batches of smoke with different optical depths (the optical depth at a particular wavelength can be estimated by multiplying the value of σ_e/M by the value of ML). The determination of the slope parameters c(λ) was done assuming RP smoke consists of phosphoric acid. This assumption is incorrect, as the burning of RP smokes apparently results in production of as yet unknown chemical species (Milham et al 1977) leading to the marked disagreement between prediction and measurement.

cannot be approximated by those of phosphoric acid [which was assumed in determination of $c(\lambda)$ in relation (5)].

HC Smoke

Compared to the highly absorbing phosphoric acid smoke, little spectral character is evident in the predicted or measured σ_e/M values for HC smoke (figures 8 and 9). The predicted values of σ_e/M have approximate $1/\lambda$ wavelength dependence in both the 3μm to 5um and 8μm to 12μm regions, as the slope parameter $c(\lambda)$ is only a slowly varying function of wavelength. Although this $1/\lambda$ dependence is borne out by the measurements in the 3μm to 5μm spectral region, for the 8μm to 12μm range the measurements show nearly neutral (wavelength independent) extinction. This markedly different spectral character for the predicted and measured extinction in the 8μm to 12μm range can be at least partially explained on the basis of errors in the $Q_e = cx$ approximation. Perusal of the Q_e versus x curves (examples of which are given in figure A-5) suggests that the relation (5) should overestimate the value of σ_e/M throughout the 8μm to 12μm spectral region (as the HC smoke particles will have size parameters predominately less than $x \approx 2$ and cancellation of errors does not occur) and the overestimate should be more at $\lambda = 8\mu m$ compared to $\lambda = 12\mu m$. Thus larger disagreement between predicted and measurement results at $\lambda = 8\mu m$ compared to $\lambda = 12\mu m$. Also, multiple scatter contributions might account for some of the discrepancy between the predicted and measured σ_e/M values in figure 9, but this is unlikely in view of the fact that the transmission has the same spectral dependence for two widely differing optical depths (the optical depths can be determined by multiplying the σ_e/M values by the value of ML, and are about 0.14 and 1.1 for the solid and dashed curves, respectively).

Fog Oil Smoke

Carlon et al[15] describe transmission measurements through petroleum oil smokes generated either by dropping oil onto a hot plate, which results in droplets with volume mean radius of about 1.7μm, or by pyrotechnic generation, which produces smaller droplets with volume mean radius of about 0.3μm.

---

[15] H. R. Carlon, D. H. Anderson, M. E. Milham, T. L. Tarnove, R. H. Frickel, and I. Sindoni, 1977, Infrared Extinction Spectra of Some Common Liquid Aerosols, Appl Opt, 16:1598-1605

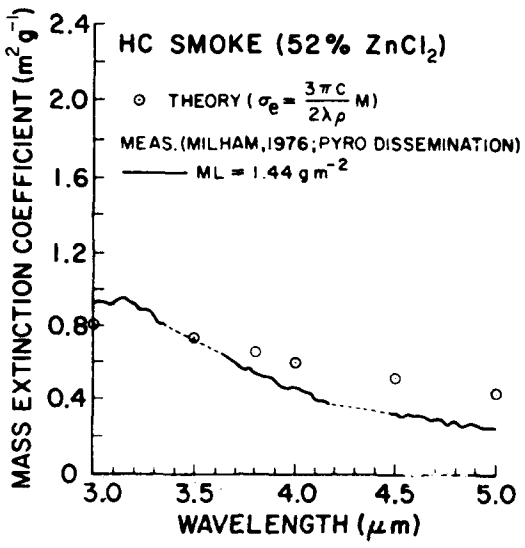

Figure 8. Ratio of aerosol extinction coefficient to mass content predicted according to the linear relation (5) (open circles), and measured by Milham (solid curve) for HC smoke disseminated by pyrotechnic. As for phosphoric acid smoke, the predicted and measured extinction has roughly $1/\lambda$ wavelength dependence in the 3μm to 5μm spectral region.

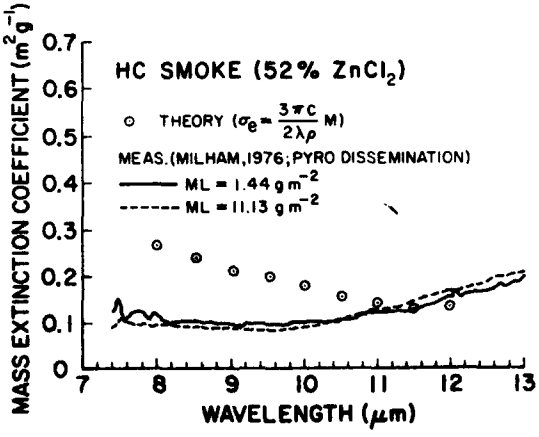

Figure 9. Same as figure 8 except for the 7μm to 13μm spectral region. The linear relation (5) (open circles) again predicts a $1/\lambda$ dependence of extinction; however, the measurements show a slight increase of extinction with wavelength. This disagreement between relation (5) and measurements is attributed to inaccuracy of the $Q_e = cx$ approximation (see text and figure A-5).

The transmission measurements for the larger fog oil droplets generated by hot plate dissemination are compared to the prediction (5) in figures 10 and 11. For the 3μm to 5μm spectral region (figure 10) the predicted σ_e/M values have roughly $1/\lambda$ wavelength dependence and are in agreement with the measurements within a factor 2. Note that the extinction measurements at the smallest optical depths in figure 10 (the optical depths range from 0.38 to 0.72 for the solid-curve measurement) are a factor 1.5 to 3 higher than those for the larger optical depths (which range from 1.8 to 3.5). Whether this difference is a reflection of multiple scatter contributions to the transmission signal at the larger optical depths (which would cause the extinction coefficient to be underestimated from the transmission measurement), or whether it is simply a reflection of the experimental errors is not known. For the 8μm to 12μm region, the $Q_e = cx$ approximation (5) overpredicts the extinction to mass ratio σ_e/M by a factor 1.2 to 4 (figure 11).

This overprediction is even more serious for smaller fog oil smoke particles as demonstrated by comparison of measured and predicted σ_e/M values in figures 12 and 13. These particles were generated by pyrotechnic dissemination and have correspondingly smaller size parameters. Thus the usefulness of relation (5) for fog oil is only marginal in the 3μm to 5μm and 8μm to 12μm IR spectral regions, as the Mie extinction efficiency is generally not well approximated by a linear function of size parameter in these wavelength regions.

FS Smoke

The final comparison of extinction to mass content σ_e/M according to relation (5) compared to measurement is for sulfuric acid mists generated by Carlon et al.[15] Their results for 38 percent sulfuric acid smoke for the λ = 0.5μm to 2.5μm, 7μm to 14μm spectral regions compared to our size-distribution-independent relation (5) are shown in figures 14 and 15. The error bars superimposed on the measurements mark the range of values obtained for several radiometer scans.* For the 7μm to 14μm spectral region, the $Q_e = cx$ approximation given by (5) is generally within error of measurement. On the other hand, the equation (5) prediction generally overestimates the measurements in the 0.55μm to 2.75μm wavelength range.

---

[15] H. R. Carlon, D. H. Anderson, M. E. Milham, T. L. Tarnove, R. H. Frickel, and I. Sindoni, 1977, Infrared Extinction Spectra of Some Common Liquid Aerosols, Appl Opt, 16:1598-1605

*H. R. Carlon, private communication, 1978

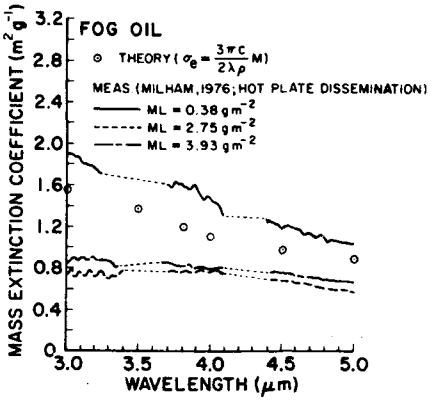

Figure 10. Ratio of aerosol extinction coefficient to mass content predicted according to the linear relation (5) (open circles) and measured by Milham (curves) for fog oil smoke generated by dropping oil onto a hot plate. The different curves are for transmission measurements made with different batches of fog oil with varying optical depth (the optical depth for a particular wavelength can be estimated by multiplying the value of σ_e/M by the value of ML). Smaller values of extinction coefficient are inferred from transmission measurements made at larger optical depths, suggesting that multiple scatter contributions may be becoming important.

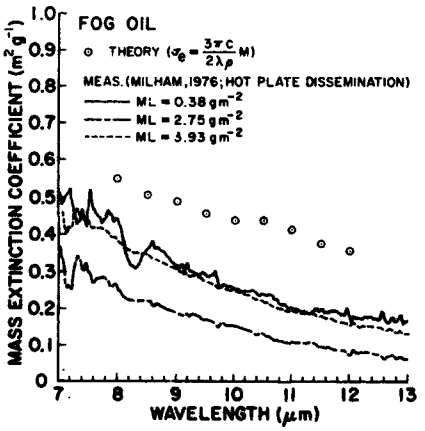

Figure 11. Same as figure 10 except for the 7μm to 13μm spectral region. The overprediction of extinction according to the linear relation (5) (open circles) is partially caused by inaccuracy of the Q_e = cx approximation (e.g., figure A-7). The good agreement of the measurements for the widely differing optical depths (solid and dashed curves) suggests multiple scatter contributions are not significant. Alternatively, experimental errors in the extinction-to-mass ratio may be so large as to obfuscate multiple scatter contributions.

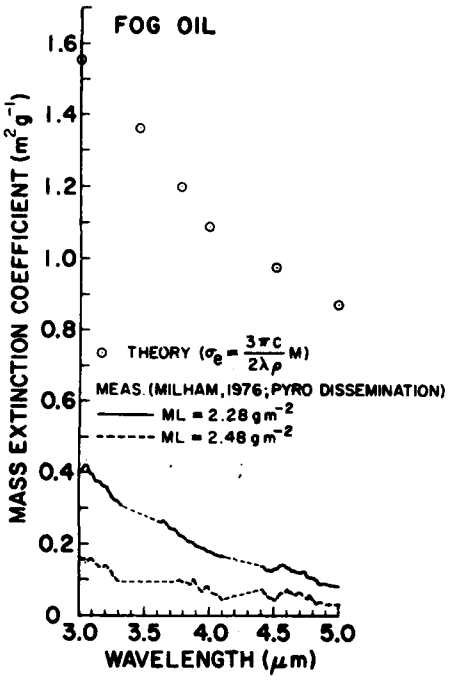

Figure 12. Ratio of extinction coefficient to mass content predicted according to the linear relation (5) (open circles) and measured by Milham (curves) for fog oil smoke generated by pyrotechnic. The measured extinction is significantly less than for the larger hot-plate generated smoke particles (e.g., figure 10). The relation (5) severely overestimates the extinction as a result of inaccuracy of the $Q_e = cx$ approximation for small particles (e.g., figure A-6).

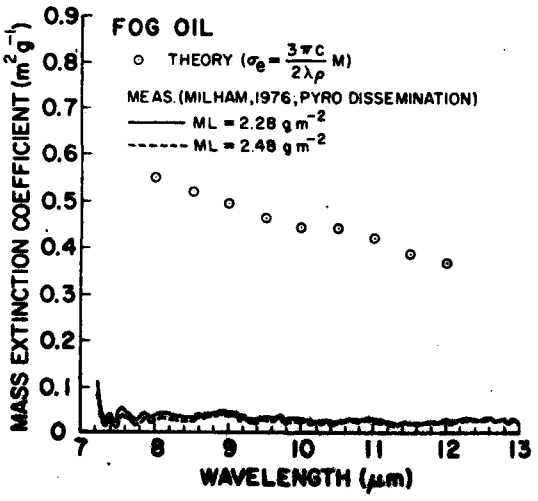

Figure 13. Same as figure 12 except for the 7μm to 13μm spectral region. Again the relation grossly overestimates extinction and its application to fog oil smoke generated by pyrotechnic is not recommended.

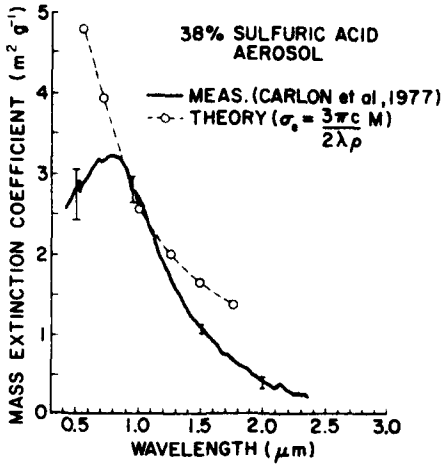

Figure 14. Values of the ratio of aerosol extinction coefficient to aerosol mass content predicted according to the size-distribution-independent linear relation (5) (open circles connected by the dashed line) and measured by Carlon et al (curve) for 38 percent sulfuric acid (62 percent water) aerosol. The linear relation (5) predicts extinction to have an approximate $1/\lambda$ wavelength dependence in the spectral region $0.55 \leq \lambda \leq 1.75\mu m$. The linear relation (5) is in best agreement with measurement at $\lambda \simeq 1\mu m$, where the maximum radius condition for these aerosols is satisfied (about 98 percent of the aerosol mass is contributed by particles with radii $r < r_m$), and particles have size parameters throughout the range $0 \leq x \leq x_m$ so that cancellation of error in the $Q_e = cx$ approximation occurs (e.g., figure 1).

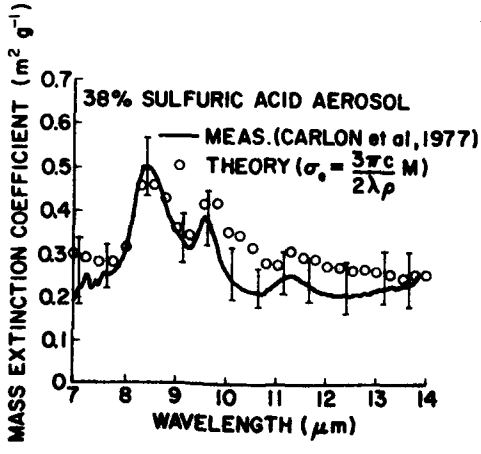

Figure 15. As in figure 14 except for $\lambda = 7\mu m$ to $14\mu m$, only in this case the theoretical points are not connected by a dashed line. In this spectral region the maximum radius condition for the linear relation (5) (open circles) to be applicable is satisfied at all wavelengths. Further, because of the relatively large imaginary index of refraction of sulfuric acid at these IR wavelengths the form of the Mie efficiency factor for extinction lends itself to be better approximated by $Q_e = cx$ than for visible or near IR wavelengths (compare figures 1 and 2). As a result the predicted relation between aerosol extinction coefficient and mass according to relation (5) is generally within error of measurement of the measured values.

The relation (5) works so well in the 7μm to 14μm spectral region as compared to the 0.55μm to 1.75μm region because: (1) the maximum radius conditions are easily satisfied at these longer wavelengths (maximum radius values are on the order of 3μm to 7μm from table A-12) as only about 2 percent of the sulfuric acid aerosol smoke mass is contributed by particles with radii $r > 1\mu m$, (2) for $r < 1\mu m$, the Mie extinction efficiency factor is accurately approximated by $Q_e = cx$ as, for example, in figure 2.

PRACTICAL APPLICATIONS OF THE $\sigma_e - M$, $\sigma_a - M$, AND $\sigma_{bs} - M$ RELATIONS

Unique relations between radiative properties of smoke aerosols and their mass content should be of considerable practical value. For example, according to the extinction-mass relation (5), the integrated mass content of smoke along a path could be determined from an IR transmission measurement between the endpoints of the path. The path must be short enough that multiple scattering effects and attenuation caused by gaseous absorption are negligible; also, forwardscatter corrections must be small.[18,19] Thus, for a CO_2 laser ($\lambda = 10.6\mu m$) transmission loss of 0.5 over a 100-m phosphoric acid (50 percent) smoke path, a path-integrated average mass content of 0.016 g m^{-3} is predicted according to relation (5) using the value of $3\pi c/2\lambda\rho$ from table A-2. Similarly, had the smoke consisted of HC (50 percent zinc chloride in water) or FS (38 percent sulfuric acid in water) rather than phosphoric acid, smoke mass contents of 0.046 g m^{-3} and 0.022 g m^{-3} would result (from values of $3\pi c/2\lambda\rho$ in tables A-7 and A-12).

An application of the relation (6) between absorption and liquid mass content of smokes would be the inference of smoke mass at a particular point in a smoke cloud from an in situ measurement of the aerosol absorption with an IR laser spectrophone. Smoke particles generally have maximum radii of 1μm to 2μm, and tables A-1 through A-13 show that the maximum radius condition for the $\sigma_a - M$ relation (6) is satisfied for most IR wavelengths considered. For example, an absorption measurement with a CO_2 laser spectrophone of 10 km^{-1} (using the value of $3\pi c/2\lambda\rho$ from tables A-3, A-8, and A-13 at $\lambda = 10.5\mu m$) corresponds to mass contents of 0.040, 0.31, and 0.054 g m^{-3} for 65 percent H_3PO_4, 65 percent $ZnCl_2$ (HC), and 75 percent sulfuric acid smokes.

---

[18] A. Deepak and M. A. Box, 1978, Forward Scattering Corrections for Optical Extinction Measurements in Aerosol Media. 1: Monodispersions, Appl Opt, 17:2900-2908

[19] A. Deepak and M. A. Box, 1978, Forward Scattering Corrections for Optical Extinction Measurements in Aerosol Media. 2: Polydispersions, Appl Opt, 17:3169-3176

The relations (5) and (6) can also be used to estimate the single scattering albedo for polydispersions of smoke particles. The albedo is defined as the ratio scattering to extinction and is an important parameter in determining the contrast obtainable by an IR sensor such as a forward looking infrared system (FLIR). From relations (5) and (6), the single scatter albedo w_o is a simple function of the slope parameters c(m) and c′(m):

$$w_o = \frac{\sigma_s}{\sigma_e} = \frac{\sigma_e - \sigma_a}{\sigma_e} = 1 - \frac{c'}{c} , \qquad (8)$$

where the refractive index m is characteristic of the smoke material at the wavelength of interest. Values of c and c′ from tables A-1 through A-13 must be substituted cautiously into equation (8) to obtain the single scatter albedo since the maximum radius conditions for the smoke particles (which are also given in the tables) must be satisfied for both extinction and absorption. However, these conditions are generally easily satisfied for all smokes considered here in the 3μm to 5μm and 8μm to 12μm spectral regions. Finally, because of the large errors involved in the $Q_e = cx$ approximation for only slightly absorbing particles, the application of equation (8) to HC, diesel oil, and fog oil smokes is not recommended when errors in the quantity $3\pi c/2\lambda\rho$ exceed 50 percent (see footnotes of tables A-1 through A-13).

The last application suggested here toward a specific DOD hardware system concerns the relation (7) between smoke backscatter coefficient and mass content. The copperhead missile seeker system sometimes relies on an Nd-YAG laser backscatter signal to find its target. If the intervening atmosphere between the missile and target contains smoke particles, the performance of the seeker system may be degraded because the backscatter signal from the smoke obscurant may obfuscate that from the target. According to relation (7) the backscatter from the smoke may be calculated directly from knowledge of the integrated smoke mass content between seeker and target (neglecting multiple scattering effects). For example, a cloud of 50 percent phosphoric acid smoke with mass loading 0.1 g m^{-3} would result in a backscatter cross section of 0.0034m^{-1} sr^{-1} at λ = 1.06μm.

COMPARISON OF EXTINCTION COEFFICIENTS OF PHOSPHORIC ACID AND HC SMOKE AT VARIOUS RELATIVE HUMIDITIES

Another application of these approximations is toward the radiative properties of hygroscopic smoke particles. Phosphoric acid and HC smoke particles are hygroscopic. They grow at the expense of atmospheric water vapor to equilibrium sizes larger than their original sizes, depending on the atmospheric temperature and relative humidity. This increase in size sometimes causes increased extinction and

obscuration. To make a comparison of the effectiveness of these two smokes, we compare their extinction coefficients as a function of relative humidity, taking into account that their mass content increases with relative humidity. We require that the initial "dry" mass contents be the same:

$$\rho_o^{(1)} V_o^{(1)} = \rho_o^{(2)} V_o^{(2)} , \tag{9}$$

where $\rho_o^{(1)}$, $\rho_o^{(2)}$ are the dry density values of the smoke materials (1) and (2) and $V_o^{(1)}$, $V_o^{(2)}$ are their initial volumes.

To predict the volume increases, we use the results of Hänel* for the fractional radius increases (r/r_o) of phosphoric acid droplets (table A-15) and HC smoke (table A-16) as a function of relative humidity f. The results are based on Hänel's original work.[20] The tables show that the fractional increase in the smoke particle radii is nearly independent of the initial particle radii. Thus we can assume to first order that the fractional radius increases r/r_o are independent of particle size, leading to the smoke volume content at relative humidity f being given by $(r/r_o)^3 v_o$. Using the approximation (5) relating extinction coefficient to aerosol mass content, we can write the extinction coefficient at relative humidity f as

$$\sigma_e(f) = \frac{3\pi c}{2\lambda} \left(\frac{r}{r_o}\right)^3 V_o . \tag{10}$$

The ratio of phosphoric acid to HC smoke extinction coefficients (under the constraint that their initial dry mass contents be the same) is then

$$\frac{\sigma_e^{(1)}}{\sigma_e^{(2)}} = \frac{c^{(1)}}{c^{(2)}} \cdot \frac{\rho_o^{(2)}}{\rho_o^{(1)}} \cdot \left[\frac{(r/r_o)^{(1)}}{(r/r_o)^{(2)}}\right]^3 . \tag{11}$$

The values of this ratio calculated for relative humidities from 40 to 95 percent at several wavelengths are given in table A-17. For relative

---

*Private communication, 1978

[20] G. Hänel, 1976, The Properties of Atmospheric Aerosol Particles as Functions of Relative Humidity at Thermodynamic Equilibrium with the Surrounding Moist Air, Adv in Geophys, 19:73-188

humidities f < 80 percent, phosphoric acid is a more effective obscurant (as it has a greater extinction coefficient) in the visible and 10.5μm to 12μm spectral regions, but less effective in the 3μm region. Results for the 4μm to 10μm spectral region have been purposely left out since we expect the $Q_e = cx$ approximation (5) to be substantially in error for HC smoke in this region. For a relative humidity of 95 percent, HC smoke is more effective at all considered wavelengths.

CONCLUSIONS

We have shown that a linear relation, independent of the form of the size distribution, should exist between volume extinction coefficient, absorption coefficient, backscatter coefficient, and mass content of several military smokes. However, the relation is valid only at particular wavelengths determined by the range of particle sizes present in the polydispersions of smoke particles. Our prediction between extinction coefficient and mass content has been compared to transmission measurements available in the literature on phosphoric acid, HC, fog oil, and FS smokes. The agreement is good (generally within 30 percent) for highly absorbing phosphoric acid and FS smoke in the 3μm to 5μm and 8μm to 12μm spectral regions, but only fair-to-poor for weakly absorbing HC and fog oil smokes (the relation overpredicts extinction by as much as a factor 2.5 for HC and 10 for fog oil generated by pyrotechnic). Four applications of our relationships between smoke aerosol extinction, absorption, backscatter, and mass content are suggested: (1) inference of path-integrated mass content of smoke from an IR laser transmissometer measurement through the smoke cloud, (2) determination of smoke mass content at a particular point in a smoke cloud from a smoke aerosol absorption measurement at that point with an IR laser spectrophone, (3) determination of smoke backscatter coefficient from knowledge of smoke mass content, and (4) prediction of the extinction coefficient of phosphoric acid and HC smoke as a function of atmospheric relative humidity.

REFERENCES

1. Charlson, R. J., N. C. Ahlquist, and H. Horvath, 1968, On the Generality of Correlation of Atmospheric Mass Concentration and Light Scatter, Atmos Environ, 2:455-464.

2. Noll, K. E., P. K. Mueller, and M. Imada, 1968, Visibility and Aerosol Concentration in Urban Air, Atmos Environ, 2:465-475.

3. Pilat, M. J., and D. S. Ensor, 1970, Plume Opacity and Particulate Mass Concentration, Atmos Environ, 4:163-173.

4. Patterson, E. M., and D. A. Gillette, 1977, Measurements of Visibility vs Mass-Concentration for Airborne Soil Particles, Atmos Environ, 11:193-196.

5. Chylek, Petr, 1975, Asymptotic Limits of the Mie-Scattering Characteristics, J Opt Soc Amer, 65:1316-1318.

6. Penndorf, R. B., 1962, Scattering and Extinction Coefficients for Small Spherical Aerosols, J Atmos Sci, 19:193.

7. Chylek, Petr, 1978, Extinction and Liquid Water Content of Fogs and Clouds, J Atmos Sci, 35:296-300.

8. Pinnick, R. G., D. L. Hoihjelle, G. Fernandez, E. B. Stenmark, J. D. Lindberg, S. G. Jennings, and G. B. Hoidale, 1978, Vertical Structure in Atmospheric Fog and Haze and Its Effects on IR and Visible Extinction, J Atmos Sci, 35:2020-2032.

9. Chylek, Petr, J. T. Kiehl, and M. K. W. Ko, 1979, Infrared Extinction and the Mass Concentration of Atmospheric Aerosols, Atmos Environ, 13:169-173.

10. Box, M. A., and B. H. J. McKellar, 1978, Direct Evaluation of Aerosol Mass Loadings from Multispectral Extinction Data, Quart J Roy Meteorol Soc, 104:755-781.

11. Querry, M. R., and I. L. Tyler, 1978, Complex Refractive Indices in the Infrared for H_3PO_4 in Water, J Opt Soc Am, 68:1404.

12. Conner, W. D., and J. R. Hodkinson, 1967, Optical Properties and Visual Effects of Smoke-Stack Plumes, US Department of Health, Education, and Welfare, Public Health Service Publication, 999-AP-30.

13. Hale, G. M., I. L. Tyler, and M. R. Querry, 1978, Complex Refractive Indices in the Infrared for Selected Oils and Alcohols, J Opt Soc Am, 68:1403.

14. Palmer, K. F., and D. Williams, 1975, Optical Constants of Sulfuric Acid: Application to the Clouds of Venus? Appl Opt, 14:208-219.

15. Carlon, H. R., D. H. Anderson, M. E. Milham, T. L. Tarnove, R. H. Frickel, and I. Sindoni, 1977, Infrared Extinction Spectra of Some Common Liquid Aerosols, Appl Opt, 16:1598-1605.

16. Milham, M. E., D. H. Anderson, R. H. Frickel, and T. L. Tarnove, 1977, New Findings on the Nature of WP/RP Smokes, Technical Report ARCSL-TR-77067, US Army ARADCOM, Chemical Systems Laboratory, Aberdeen Proving Ground, MD.

17. Milham, M. E., 1976, A Catalog of Optical Extinction Data for Various Aerosols/Smokes, Report ED-SP-77002, Edgewood Arsenal, Aberdeen Proving Ground, MD.

18. Deepak, A., and M. A. Box, 1978, Forward Scattering Corrections for Optical Extinction Measurements in Aerosol Media. 1: Monodispersions, Appl Opt, 17, 2900-2908.

19. Deepak, A., and M. A. Box, 1978, Forward Scattering Corrections for Optical Extinction Measurements in Aerosol Media. 2: Polydispersions, Appl Opt, 17:3169-3176.

20. Hanel, G., 1976, The Properties of Atmospheric Aerosol Particles as Functions of Relative Humidity at Thermodynamic Equilibrium with the Surrounding Moist Air, Adv in Geophys, 19:73-188.

SELECTED BIBLIOGRAPHY

Pinnick, R. G., S. G. Jennings, Petr Chýlek, and H. J. Auvermann, 1979, Verification of a Linear Relation Between IR Extinction, Absorption and Liquid Water Content of Fogs, J Atmos Sci, 36:1577-1586.

APPENDIX. FIGURES A-1 THROUGH A-10 AND TABLES A-1 THROUGH A-17

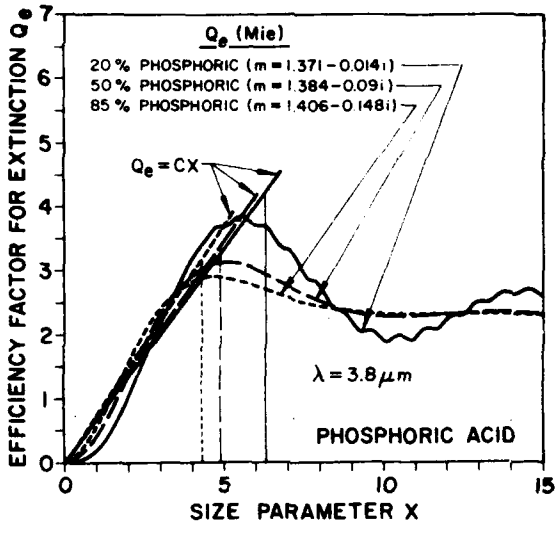

Figure A-1. Efficiency factors for extinction Q_e for phosphoric acid droplets at a wavelength $\lambda = 3.8\mu m$, and their approximation by straight lines $Q_e(x) = cx$. The efficiency factors are well approximated by the straight lines up to some maximum size parameter (indicated by the vertical lines).

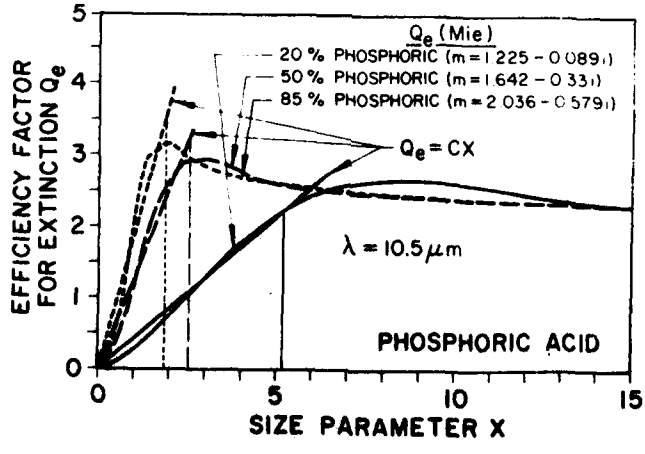

Figure A-2. Same as figure A-1 only for $\lambda = 10.5\mu m$. Note the slope parameter c is a sensitive function of the phosphoric acid content of the droplets.

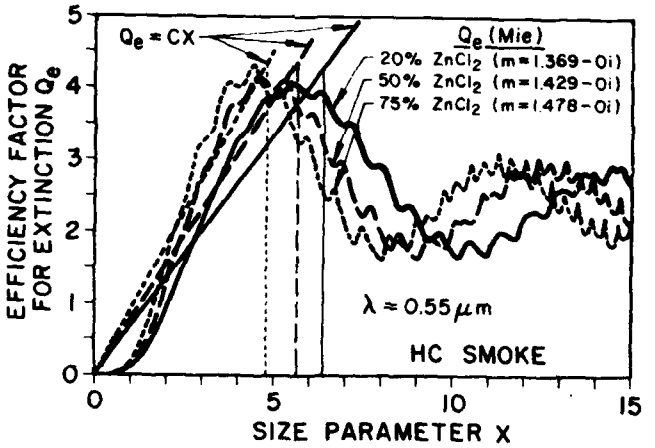

Figure A-3. Same as figure A-1 only for HC smoke droplets at a wavelength $\lambda = 0.55\mu m$. In this case particles must have size parameters $x \lesssim 6$ (corresponding to radii $r \lesssim 0.5\mu m$) for the $Q_e = cx$ approximation to apply. Since HC smoke particles generally violate this condition (e.g., Milham 1976, reports size distributions of HC smoke having mass mean radii of $0.66\mu m$), the linear relation (5) will probably overestimate extinction at $\lambda = 0.55\mu m$.

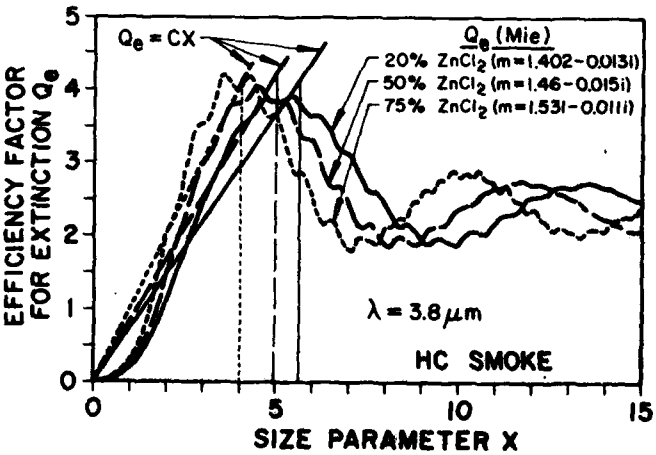

Figure A-4. Same as figure A-3 except for a wavelength $\lambda = 3.8\mu m$. At this longer wavelength the maximum radius condition is for particles with radii $r \gtrsim 3\mu m$ (corresponding to $x \gtrsim 5$) and should be satisfied for HC smoke particles. However, even though this condition is satisfied, the $Q_e = cx$ approximation is not very accurate, as the Mie efficiencies are significantly overestimated for $x \lesssim 2$ and underestimated for $2 \lesssim x \lesssim 5$. Thus, for the linear relation (5) to be a good approximation we must have particles with size parameters throughout the range $0 \lesssim x \lesssim 5$ (corresponding to radii $0 \lesssim r \lesssim 3\mu m$) so that cancellation of errors can occur.

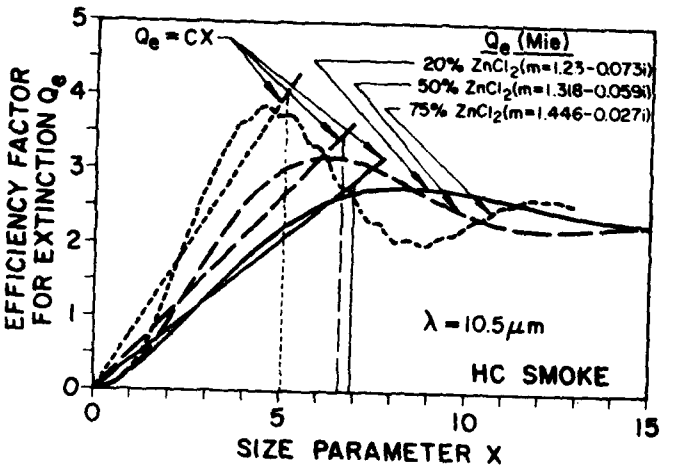

Figure A-5. Same as figure A-3 except for a wavelength $\lambda = 10.5\mu m$. At this wavelength the maximum radius condition for the $Q_e = cx$ approximations should be easily satisfied ($r_m \tilde{=} 10\mu m$ corresponds to $x_m \tilde{=} 6$). But because HC smoke particles will have size parameters less than $x \tilde{=} 2$ at this wavelength, the $Q_e = cx$ approximation overestimates extinction and the linear relation (5) is not expected to be very accurate.

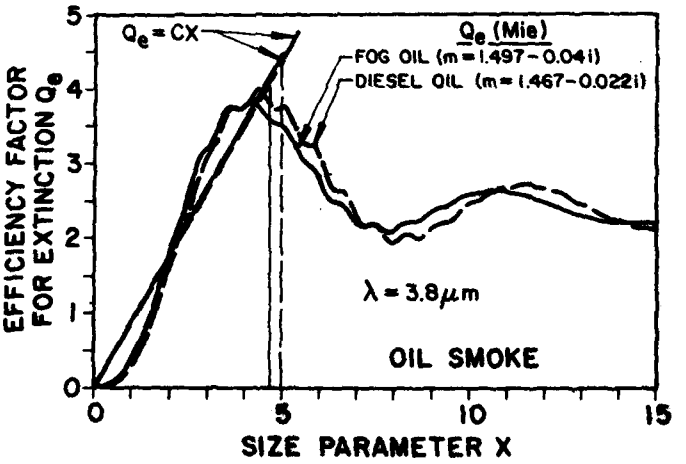

Figure A-6. Efficiency factors for extinction Q_e for fog oil and diesel oil droplets at a wavelength $\lambda = 3.8\mu m$, and their approximation by straight lines $Q_e(x) = cx$ for $x \lesssim 5$. As for HC smoke at this wavelength, the $Q_e = cx$ approximation is not very accurate, as the Mie efficiencies are grossly overestimated for $x \lesssim 2$ and underestimated for $2 \lesssim x \lesssim 5$. Hence for the linear relation (5) between extinction and mass content to be applicable we must have particles with radii throughout the range $0 \lesssim r \lesssim 3\mu m$ (corresponding to $0 \lesssim x \lesssim 5$) so that cancellation of errors can occur.

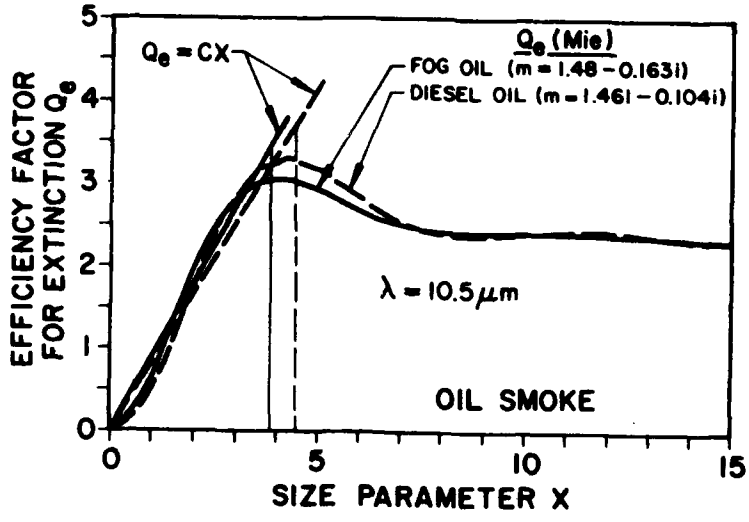

Figure A-7. Same as figure A-6 except for λ = 10.5μm.

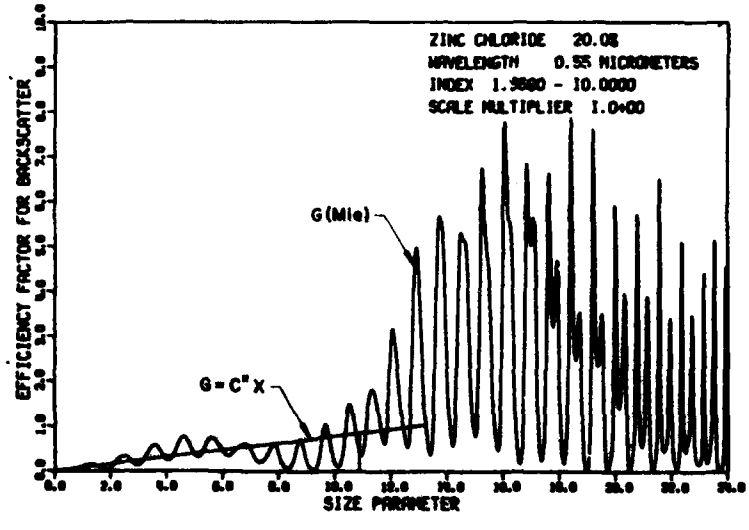

Figure A-8. Normalized backscatter gain G for 20 percent zinc chloride (in water) droplets at the wavelength λ = 0.55μm and its approximation by a straight line G(x) = c"x for x < 11. The approximation overestimates the exact value of G at some size parameters x, but underestimates it at others (still with x < 11). These two errors tend to cancel out in the evaluation of the integral in equation (3). This approximation leads to the linear relation (7) between backscatter coefficient and aerosol mass content, which is independent of the particle size distribution.

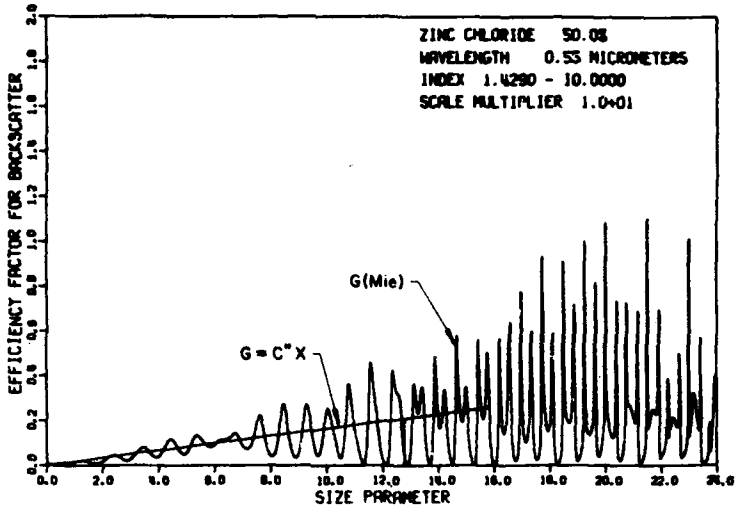

Figure A-9. Same as figure A-8 except for 50 percent zinc chloride in water.

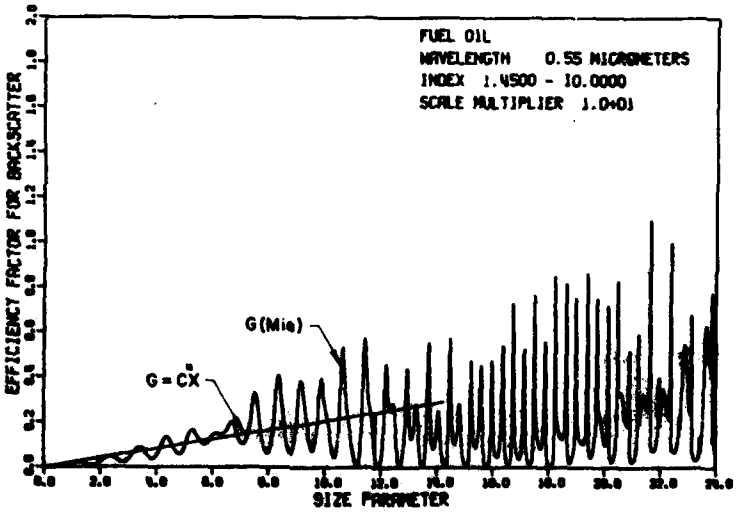

Figure A-10. Same as figure A-8 except for fuel oil.

TABLE A-1. 20 PERCENT ORTHOPHOSPHORIC ACID IN WATER
(density $\rho = 1.1134$ g cm^{-3})

At a given wavelength λ the efficiency factor for extinction Q_e (and absorption Q_a) for phosphoric acid smokes can be approximated by a linear function of size parameter $Q_e = cx$ (or $Q_a = c'x$) for size parameters $x \leq x_m$, or equivalently for particle radii $r \leq r_m$. The values of r_m and c (and c') are determined from the efficiency curves (see for example figure A-1). If a polydispersion of phosphoric acid droplets has particles with radii $r \leq r_m(\lambda)$, from the table we can find the wavelengths for which a linear relationship between extinction (or absorption) and aerosol mass content exists, and the appropriate value of the parameter c (or c'). The value of the quantity $3\pi c/2\lambda\rho$ (or $3\pi c'/2\lambda\rho$) multiplied by the smoke mass content M gives the extinction coefficient σ_e (or absorption coefficient σ_a). Also given in the table is the ratio of the absorption to the extinction coefficient σ_a/σ_e. The single-scatter albedo $w_o = 1 - \sigma_a/\sigma_e$.

	Extinction			Absorption			
λ(μm)	c	r_m(μm)	$\frac{3\pi c}{2\lambda\rho}$($m^2g^{-1}$)	c'	r_m(μm)	$\frac{3\pi c'}{2\lambda\rho}$($m^2g^{-1}$)	σ_a/σ_e
0.55	0.69	0.52	5.3 c				
1.06	0.69	1.0	2.7 c				
3.0	0.76	1.9	1.1 a	0.59	1.1	0.84 a	0.78
3.5	0.76	3.1	0.92c	0.088	4.9	0.11 a	0.12
3.8	0.67	3.8	0.75c	0.054	5.8	0.060a	0.08
4.0	0.67	4.0	0.71c	0.058	6.8	0.061a	0.09
4.5	-	-	-	0.068	8.0	0.064a	-
5.0	-	-	-	0.074	6.4	0.063a	-
8.0	0.53	7.3	0.28c	0.14	10.0	0.076a	0.27
8.5	0.52	7.2	0.26c	0.18	8.7	0.088a	0.34
9.0	0.49	8.4	0.23c	0.16	10.0	0.074a	0.32
9.5	0.45	8.7	0.20b	0.17	10.1	0.077a	0.38
10.0	0.48	7.7	0.20a	0.24	8.4	0.099a	0.49
10.5	0.43	8.6	0.17a	0.20	10.0	0.081a	0.47
11.0	0.40	7.4	0.15a	0.26	7.9	0.10 a	0.66
11.5	0.44	6.9	0.16a	0.33	6.3	0.12 a	0.76
12.0	0.50	7.3	0.18a	0.42	5.4	0.15 a	0.85

a - Error in $3\pi c/2\lambda\rho$ (or $3\pi c'/2\lambda\rho$) is estimated to be less than 30 percent.
b - Error in $3\pi c/2\lambda\rho$ (or $3\pi c'/2\lambda\rho$) is estimated to be less than 50 percent.
c - Error in $3\pi c/2\lambda\rho$ (or $3\pi c'/2\lambda\rho$) is estimated to be less than 100 percent.

TABLE A-2. 50 PERCENT ORTHOPHOSPHORIC ACID IN WATER

(density $\rho = 1.335$ g cm^{-3})

	Extinction			Absorption			
$\lambda(\mu m)$	c	$r_m(\mu m)$	$\frac{3\pi c}{2\lambda\rho}(m^2g^{-1})$	c'	$r_m(\mu m)$	$\frac{3\pi c'}{2\lambda\rho}(m^2g^{-1})$	σ_a/σ_e
0.55	0.72	0.50	4.7 c				
1.06	0.72	0.96	2.4 c				
3.0	0.62	2.2	0.74 a	0.39	1.4	0.46 a	0.63
3.5	0.68	2.7	0.68 b	0.30	2.2	0.30 a	0.43
3.8	0.70	3.0	0.64 b	0.25	2.9	0.23 a	0.35
4.0	0.66	3.3	0.58 b	0.24	3.1	0.21 a	0.36
4.5	0.69	3.6	0.54 b	0.24	4.0	0.19 a	0.35
5.0	0.65	4.2	0.46 b	0.21	4.6	0.15 a	0.33
8.0	0.58	5.0	0.26 a	0.40	4.4	0.18 a	0.69
8.5	0.72	4.0	0.30 a	0.54	4.1	0.22 a	0.74
9.0	0.79	4.2	0.31 a	0.52	4.3	0.20 a	0.66
9.5	0.93	2.9	0.35 a	0.83	2.2	0.31 a	0.89
10.0	1.59	2.7	0.56 a	1.41	1.6	0.50 a	0.89
10.5	1.30	4.3	0.43 a	0.70	4.3	0.24 a	0.54
11.0	1.05	5.2	0.34 a	0.53	5.5	0.17 a	0.51
11.5	1.00	5.9	0.31 a	0.52	5.7	0.16 a	0.52
12.0	0.92	6.2	0.27 a	0.48	6.4	0.14 a	0.52

a - Error in $3\pi c/2\lambda\rho$ (or $3\pi c'/2\lambda\rho$) is estimated to be less than 30 percent.
b - Error in $3\pi c/2\lambda\rho$ (or $3\pi c'/2\lambda\rho$) is estimated to be less than 50 percent.
c - Error in $3\pi c/2\lambda\rho$ (or $3\pi c'/2\lambda\rho$) is estimated to be less than 100 percent.

TABLE A-3. 65 PERCENT ORTHOPHOSPHORIC ACID IN WATER

(density ρ = 1.475 g cm^{-3})

	Extinction			Absorption			
$\lambda(\mu m)$	c	$r_m(\mu m)$	$\frac{3\pi c}{2\lambda\rho}(m^2 g^{-1})$	c'	$r_m(\mu m)$	$\frac{3\pi c'}{2\lambda\rho}(m^2 g^{-1})$	σ_a/σ_e
0.55	0.83	0.44	4.8 c				
1.06	0.83	0.85	2.5 c				
3.0	0.58	2.5	0.61a	0.33	1.7	0.34a	0.56
3.5	0.68	2.6	0.62a	0.35	2.0	0.32a	0.52
3.8	0.70	2.9	0.59a	0.31	2.3	0.26a	0.45
4.0	0.67	3.1	0.54a	0.29	2.7	0.23a	0.43
4.5	0.72	3.3	0.51b	0.29	3.3	0.20a	0.40
5.0	0.67	3.9	0.43b	0.25	4.6	0.16a	0.37
8.0	0.62	4.0	0.25a	0.47	3.5	0.19a	0.76
8.5	0.85	3.3	0.32a	0.70	3.0	0.26a	0.82
9.0	0.93	3.7	0.33a	0.73	3.3	0.26a	0.78
9.5	1.39	2.2	0.47a	1.28	1.6	0.43a	0.92
10.0	1.93	2.5	0.62a	1.66	1.6	0.53a	0.86
10.5	1.59	3.7	0.48b	0.83	4.0	0.25a	0.52
11.0	1.31	4.4	0.38b	0.65	5.0	0.19a	0.50
11.5	1.25	4.9	0.35b	0.59	5.7	0.17a	0.47
12.0	1.16	5.4	0.31b	0.55	5.9	0.15a	0.48

a - Error in $3\pi c/2\lambda\rho$ (or $3\pi c'/2\lambda\rho$) is estimated to be less than 30 percent.
b - Error in $3\pi c/2\lambda\rho$ (or $3\pi c'/2\lambda\rho$) is estimated to be less than 50 percent.
c - Error in $3\pi c/2\lambda\rho$ (or $3\pi c'/2\lambda\rho$) is estimated to be less than 100 percent.

TABLE A-4. 85 PERCENT ORTHOPHOSPHORIC ACID IN WATER

(density $\rho = 1.689$ g cm^{-3})

	Extinction			Absorption			
$\lambda(\mu m)$	c	$r_m(\mu m)$	$\frac{3\pi c}{2\lambda\rho}(m^2 g^{-1})$	c'	$r_m(\mu m)$	$\frac{3\pi c'}{2\lambda\rho}(m^2 g^{-1})$	σ_a/σ_e
0.55	0.86	0.42	4.4 c				
1.06	0.86	0.81	2.3 c				
3.0	0.55	2.7	0.51a	0.25	2.0	0.23a	0.46
3.5	0.70	2.3	0.56a	0.42	1.7	0.33a	0.60
3.8	0.75	2.6	0.55a	0.36	2.2	0.27a	0.49
4.0	0.70	2.9	0.49a	0.36	2.2	0.25a	0.51
4.5	0.75	3.1	0.47b	0.33	3.3	0.21a	0.44
5.0	0.72	3.7	0.40b	0.29	3.8	0.16a	0.40
8.0	0.69	3.2	0.24a	0.57	3.2	0.20a	0.83
8.5	1.06	2.6	0.35a	0.83	2.8	0.27a	0.78
9.0	1.34	2.4	0.41a	1.01	2.6	0.31a	0.75
9.5	2.17	1.7	0.64a	1.82	1.4	0.53a	0.84
10.0	2.36	2.1	0.66a	2.04	1.4	0.57a	0.87
10.5	1.90	3.0	0.50b	1.22	2.7	0.32a	0.64
11.0	1.65	3.9	0.42b	0.87	3.4	0.22a	0.53
11.5	1.54	4.2	0.37b	0.80	3.8	0.19b	0.52
12.0	1.39	4.9	0.33b	0.61	5.9	0.14a	0.44

a - Error in $3\pi c/2\lambda\rho$ (or $3\pi c'/2\lambda\rho$) is estimated to be less than 30 percent.
b - Error in $3\pi c/2\lambda\rho$ (or $3\pi c'/2\lambda\rho$) is estimated to be less than 50 percent.
c - Error in $3\pi c/2\lambda\rho$ (or $3\pi c'/2\lambda\rho$) is estimated to be less than 100 percent.

TABLE A-5. 20 PERCENT ZINC CHLORIDE IN WATER (HC SMOKE)
(density $\rho = 1.1866$ g cm^{-3})

At a given wavelength λ the efficiency factor for extinction Q_e (and absorption Q_a) for HC smoke aerosols can be approximated by a linear function of size parameter $Q_e = cx$ (or $Q_a = c'x$) for size parameters $x \leq x_m$ or equivalently for particle radii $r \leq r_m$. The values of r_m and c (and c') are determined from the efficiency curves (see for example figures A-3 through A-5). If a polydispersion of HC smoke droplets has particles with radii $r \leq r_m(\lambda)$, from the table we can find the wavelengths for which a linear relationship between extinction (or absorption) and aerosol mass content exists, and the appropriate value of the parameter c (or c'). The value of the quantity $3\pi c/2\lambda\rho$ (or $3\pi c'/2\lambda\rho$) multiplied by the smoke mass content M gives the extinction coefficient σ_e (or obsorption coefficient σ_a). Also given in the table is the ratio of the absorption to the extinction coefficient σ_a/σ_e. The single-scatter albedo $w_o = 1 - \sigma_a/\sigma_e$.

	Extinction			Absorption			
λ(μm)	c	r_m(μm)	$\frac{3\pi c}{2\lambda\rho}$(m^{2}g^{-1})	c'	r_m(μm)	$\frac{3\pi c'}{2\lambda\rho}$(m^{2}g^{-1})	σ_a/σ_e
0.55	0.68	0.51	4.9 c				
1.06	0.68	0.98	2.5 c				
3.0	0.81	1.9	1.1 a	0.46	1.6	0.64 a	0.79
3.5	0.80	2.9	0.91c	0.086	5.9	0.10 a	0.12
3.8	0.75	3.8	0.78c	0.051	7.7	0.053a	0.07
4.0	0.72	3.8	0.72c	0.050	8.4	0.050a	0.07
4.5	-	-	-	0.070	8.3	0.062a	-
5.0	-	-	-	0.070	8.9	0.056a	-
8.0	-	-	-	0.12	11.9	0.058a	-
8.5	-	-	-	0.12	12.7	0.060a	-
9.0	-	-	-	0.13	11.9	0.058a	-
9.5	-	-	-	0.14	11.7	0.058a	-
10.0	0.45	12.0	0.18c	0.15	10.8	0.059a	0.33
10.5	0.41	11.6	0.15b	0.18	9.6	0.067a	0.43
11.0	0.39	10.2	0.14a	0.22	9.1	0.078a	0.56
11.5	0.40	10.6	0.13a	0.28	7.8	0.097a	0.70
12.0	0.47	8.6	0.15a	0.37	6.3	0.12 a	0.80

a - Error in $3\pi c/2\lambda\rho$ (or $3\pi c'/2\lambda\rho$) is estimated to be less than 30 percent.
b - Error in $3\pi c/2\lambda\rho$ (or $3\pi c'/2\lambda\rho$) is estimated to be less than 50 percent.
c - Error in $3\pi c/2\lambda\rho$ (or $3\pi c'/2\lambda\rho$) is estimated to be less than 100 percent.

TABLE A-6. 40 PERCENT ZINC CHLORIDE IN WATER

(density ρ = 1.4173 g cm^{-3})

	Extinction			Absorption			
$\lambda(\mu m)$	c	$r_m(\mu m)$	$\frac{3\pi c}{2\lambda\rho}(m^2g^{-1})$	c'	$r_m(\mu m)$	$\frac{3\pi c'}{2\lambda\rho}(m^2g^{-1})$	σ_a/σ_e
0.55	0.76	0.47	4.6 c				
1.06	0.76	0.91	2.4 c				
3.0	0.85	1.7	0.95a	0.40	1.9	0.44 a	0.47
3.5	0.86	2.7	0.82c	0.093	5.4	0.088a	0.10
3.8	0.82	3.2	0.72c	0.049	7.7	0.043a	0.052
4.0	0.80	3.4	0.66c	0.043	8.4	0.036a	0.054
4.5	-	-	-	0.064	8.7	0.048a	-
5.0	-	-	-	0.066	9.6	0.044a	-
8.0	-	-	-	0.11	11.9	0.046a	-
8.5	-	-	-	0.12	12.6	0.048a	-
9.0	-	-	-	0.12	12.4	0.046a	-
9.5	-	-	-	0.14	11.3	0.048a	-
10.0	-	-	-	0.16	10.4	0.054a	-
10.5	0.51	10.8	0.16c	0.18	10.7	0.056a	0.35
11.0	0.46	11.1	0.14b	0.21	9.3	0.064a	0.46
11.5	0.46	10.3	0.13a	0.26	8.4	0.075a	0.57
12.0	0.48	10.0	0.13a	0.33	7.4	0.092a	0.69

a - Error in $3\pi c/2\lambda\rho$ (or $3\pi c'/2\lambda\rho$) is estimated to be less than 30 percent.
b - Error in $3\pi c/2\lambda\rho$ (or $3\pi c'/2\lambda\rho$) is estimated to be less than 50 percent.
c - Error in $3\pi c/2\lambda\rho$ (or $3\pi c'/2\lambda\rho$) is estimated to be less than 100 percent.

TABLE A-7. 50 PERCENT ZINC CHLORIDE IN WATER

(density ρ = 1.5681 g cm^{-3})

	Extinction			Absorption			
$\lambda(\mu m)$	c	$r_m(\mu m)$	$\frac{3\pi c}{2\lambda\rho}(m^2 g^{-1})$	c'	$r_m(\mu m)$	$\frac{3\pi c'}{2\lambda\rho}(m^2 g^{-1})$	σ_a/σ_e
0.55	0.78	0.46	4.3 c				
1.06	0.78	0.89	2.2 c				
3.0	0.81	1.9	0.81a	0.47	1.4	0.47 a	0.58
3.5	0.89	2.6	0.76c	0.12	3.5	0.10 a	0.14
3.8	0.86	3.0	0.68c	0.061	6.3	0.048a	0.07
4.0	0.83	3.3	0.62c	0.059	5.3	0.044a	0.07
4.5	-	-	-	0.058	6.2	0.039a	-
5.0	-	-	-	0.066	5.8	0.040a	-
8.0	-	-	-	0.099	10.8	0.037a	-
8.5	-	-	-	0.11	11.8	0.038a	-
9.0	-	-	-	0.13	9.7	0.042a	-
9.5	-	-	-	0.13	11.2	0.043a	-
10.0	-	-	-	0.15	11.1	0.044a	-
10.5	0.53	11.0	0.15c	0.17	10.3	0.048a	0.32
11.0	0.52	11.6	0.14b	0.19	10.0	0.053a	0.37
11.5	0.48	11.5	0.13a	0.24	7.9	0.063a	0.50
12.0	0.51	9.5	0.13a	0.31	7.1	0.078a	0.61

a - Error in $3\pi c/2\lambda\rho$ (or $3\pi c'/2\lambda\rho$) is estimated to be less than 30 percent.
b - Error in $3\pi c/2\lambda\rho$ (or $3\pi c'/2\lambda\rho$) is estimated to be less than 50 percent.
c - Error in $3\pi c/2\lambda\rho$ (or $3\pi c'/2\lambda\rho$) is estimated to be less than 100 percent.

TABLE A-8. 65 PERCENT ZINC CHLORIDE IN WATER

(density $\rho = 1.851$ g cm^{-3})

	Extinction			Absorption			
λ(μm)	c	r_m(μm)	$\frac{3\pi c}{2\lambda\rho}$(m^{2}g^{-1})	c'	r_m(μm)	$\frac{3\pi c'}{2\lambda\rho}$(m^{2}g^{-1})	σ_a/σ_e
0.55	0.88	0.40	4.1 c				
1.06	0.88	0.77	2.1 c				
3.0	0.95	0.96	0.80a	0.43	1.6	0.36 a	0.45
3.5	1.00	2.4	0.73c	0.087	4.3	0.063a	0.09
3.8	0.97	2.8	0.65c	0.039	5.2	0.026a	0.04
4.0	0.92	3.0	0.59c	0.025	7.4	0.016a	0.03
4.5	-	-	-	0.037	7.1	0.021a	-
5.0	-	-	-	0.045	6.9	0.023a	-
8.0	-	-	-	0.095	9.5	0.030a	-
8.5	-	-	-	0.11	9.0	0.034a	-
9.0	-	-	-	0.11	10.9	0.032a	-
9.5	-	-	-	0.099	12.5	0.027a	-
10.0	-	-	-	0.12	11.9	0.031a	-
10.5	-	-	-	0.13	12.3	0.032a	-
11.0	-	-	-	0.15	12.3	0.034a	-
11.5	0.59	10.9	0.13c	0.17	11.3	0.047a	0.29
12.0	0.56	10.1	0.12b	0.24	9.2	0.050a	0.42

a ~ Error in $3\pi c/2\lambda\rho$ (or $3\pi c'/2\lambda\rho$) is estimated to be less than 30 percent.
b ~ Error in $3\pi c/2\lambda\rho$ (or $3\pi c'/2\lambda\rho$) is estimated to be less than 50 percent.
c ~ Error in $3\pi c/2\lambda\rho$ (or $3\pi c'/2\lambda\rho$) is estimated to be less than 100 percent.

TABLE A-9. 75 PERCENT ZINC CHLORIDE IN WATER

(density ρ = 2.06 g cm^{-3})

	Extinction			Absorption			
λ(μm)	c	r_m(μm)	$\frac{3\pi c}{2\lambda\rho}(m^2g^{-1})$	c'	r_m(μm)	$\frac{3\pi c'}{2\lambda\rho}(m^2g^{-1})$	σ_a/σ_e
0.55	0.91	0.40	3.8 c				
1.06	0.91	0.77	2.0 c				
3.0	1.01	1.4	0.77b	0.43	1.7	0.33 a	0.42
3.5	1.04	2.2	0.68c	0.086	4.2	0.056a	0.08
3.8	1.04	2.4	0.62c	0.053	5.3	0.032a	0.05
4.0	1.02	2.7	0.58c	0.030	6.8	0.017a	0.03
4.5	-	-	-	0.035	6.8	0.018a	-
5.0	-	-	-	0.046	7.3	0.021a	-
8.0	-	-	-	0.066	9.6	0.019a	-
8.5	-	-	-	0.087	10.8	0.023a	-
9.0	-	-	-	0.10	11.8	0.026a	-
9.5	-	-	-	0.10	13.2	0.024a	-
10.0	-	-	-	0.12	11.4	0.028a	-
10.5	-	-	-	0.10	13.7	0.022a	-
11.0	-	-	-	0.083	13.6	0.027a	-
11.5	-	-	-	0.080	16.5	0.016a	-
12.0	-	-	-	0.16	11.0	0.030a	-

a - Error in $3\pi c/2\lambda\rho$ (or $3\pi c'/2\lambda\rho$) is estimated to be less than 30 percent.
b - Error in $3\pi c/2\lambda\rho$ (or $3\pi c'/2\lambda\rho$) is estimated to be less than 50 percent.
c - Error in $3\pi c/2\lambda\rho$ (or $3\pi c'/2\lambda\rho$) is estimated to be less than 100 percent.

TABLE A-10. 100 PERCENT DIESEL FUEL OIL

(density $\rho = 0.8419$ g m^{-3})

At a given wavelength λ the efficiency factor for extinction Q_e (and absorption Q_a) for diesel fuel oil aerosols can be approximated by a linear function of size parameter $Q_e = cx$ (or $Q_a = c'x$) for size parameters $x \leq x_m$ or equivalently for particle radii $r \leq r_m$. The values of r_m and c (and c') are determined from the efficiency curves (see for example figures A-6 through A-7). If a polydispersion of oil droplets has particles with radii $r \leq r_m(\lambda)$, from the table we can find the wavelengths for which a linear relationship between extinction (or absorption) and aerosol mass content exists, and the appropriate value of the parameter c (or c'). The value of the quantity $3\pi c/2\lambda\rho$ (or $3\pi c'/2\lambda\rho$) multiplied by the smoke or oil mass content M gives the extinction coefficient σ_e (or absorption coefficient σ_a). Also given in the table is the ratio of the absorption to the extinction coefficient σ_a/σ_e. The single-scatter albedo $w_o = 1 - \sigma_a/\sigma_e$.

	Extinction			Absorption			
$\lambda(\mu m)$	c	$r_m(\mu m)$	$\frac{3\pi c}{2\lambda\rho}(m^2g^{-1})$	c'	$r_m(\mu m)$	$\frac{3\pi c'}{2\lambda\rho}(m^2g^{-1})$	σ_a/σ_e
0.55	0.84	0.4	7.9c				
1.06	0.84	0.8	4.1c				
3.0	0.83	2.5	1.5c	0.049	6.8	0.092a	0.06
3.5	0.92	2.3	1.5c	0.24	3.1	0.38 a	0.26
3.8	0.87	3.0	1.3c	0.086	3.8	0.13 a	0.10
4.0	0.86	3.1	1.2c	0.087	5.6	0.12 a	0.10
4.5	-	-	-	0.12	5.6	0.15 a	-
5.0	-	-	-	0.15	5.2	0.16 a	-
8.0	-	-	-	0.23	6.8	0.16 a	-
8.5	-	-	-	0.24	7.4	0.16 a	-
9.0	-	-	-	0.26	6.8	0.16 a	-
9.5	-	-	-	0.26	8.1	0.15 a	-
10.0	-	-	-	0.28	8.3	0.16 a	-
10.5	-	-	-	0.28	8.4	0.15 a	-
11.0	-	-	-	0.27	9.1	0.14 a	-
11.5	-	-	-	0.25	10.1	0.12 a	-
12.0	-	-	-	0.27	9.2	0.13 a	-

a - Error in $3\pi c/2\lambda\rho$ (or $3\pi c'/2\lambda\rho$) is estimated to be less than 30 percent.
c - Error in $3\pi c/2\lambda\rho$ (or $3\pi c'/2\lambda\rho$) is estimated to be less than 100 percent.

TABLE A-11. 100 PERCENT PALE OIL (FOG OIL)
(density $\rho = 0.914$ g cm^{-3})

At a given wavelength λ the efficiency factor for extinction Q_e (and absorption Q_a) for fog oil aerosols can be approximated by a linear function of size parameter $Q_e = cx$ (or $Q_a = c'x$) for size parameters $x \leq x_m$ or equivalently for particle radii $r \leq r_m$. The values of r_m and c (and c') are determined from the efficiency curves (see for example figures A-6 through A-7). If a polydispersion of oil droplets has particles with radii $r \leq r_m(\lambda)$, from the table we can find the wavelengths for which a linear relationship between extinction (or absorption) and aerosol mass content exists, and the appropriate value of the parameter c (or c'). The value of the quantity $3\pi c/2\lambda\rho$ (or $3\pi c'/2\lambda\rho$) multiplied by the smoke or oil mass content M gives the extinction coefficient σ_e (or absorption coefficient σ_a). Also given in the table is the ratio of the absorption to the extinction coefficient σ_a/σ_e. The single-scatter albedo $w_o = 1 - \sigma_a/\sigma_e$.

	Extinction			Absorption			
λ(μm)	c	r_m(μm)	$\frac{3\pi c}{2\lambda\rho}$(m^{2}g^{-1})	c'	r_m(μm)	$\frac{3\pi c'}{2\lambda\rho}$(m^{2}g^{-1})	σ_a/σ_e
0.55	0.84	0.43	7.9c				
1.06	0.84	0.83	4.1c				
3.0	0.91	2.2	1.6c	0.094	4.5	0.16a	0.10
3.5	0.93	2.4	1.4c	0.26	3.9	0.39a	0.29
3.8	0.89	2.8	1.2c	0.15	2.7	0.20a	0.17
4.0	-	-	-	0.56	4.0	0.20a	-
4.5	-	-	-	0.16	4.6	0.22a	-
5.0	-	-	-	0.23	4.6	0.23a	-
8.0	0.85	5.7	0.55c	0.34	5.1	0.22a	0.39
8.5	0.85	5.7	0.51c	0.34	5.6	0.20a	0.40
9.0	0.85	6.1	0.49c	0.35	6.0	0.20a	0.41
9.5	0.84	6.5	0.46c	0.36	6.6	0.20a	0.43
10.0	0.85	6.3	0.44c	0.40	6.1	0.20a	0.46
10.5	0.89	6.5	0.44c	0.38	7.0	0.18a	0.42
11.0	0.89	6.8	0.42c	0.37	7.4	0.17a	0.41
11.5	0.86	7.4	0.38c	0.36	7.6	0.15a	0.42
12.0	0.84	7.4	0.36c	0.39	7.2	0.17a	0.47

a - Error in $3\pi c/2\lambda\rho$ (or $3\pi c'/2\lambda\rho$) is estimated to be less than 30 percent.
c - Error in $3\pi c/2\lambda\rho$ (or $3\pi c'/2\lambda\rho$) is estimated to be less than 100 percent, not recommended for application to fog oil smoke generated by pyrotechnic.

TABLE A-12. 38 PERCENT SULFURIC ACID IN WATER

(density $\rho = 1.286$ g cm^{-3})

At a given wavelength λ the efficiency factor for extinction Q_e (and absorption Q_a) for sulfuric acid aerosols can be approximated by a linear function of size parameter $Q_e = cx$ (or $Q_a = c'x$) for size parameter $x \leq x_m$ or equivalently for particle radii $r \leq r_m$. The values of r_m and c (and c') are determined from the efficiency curves (see for example figures 1 and 2). If a polydispersion of sulfuric acid droplets has particles with radii $r \leq r_m(\lambda)$, from the table we can find the wavelengths for which a linear relationship between extinction (or absorption) and aerosol mass content exists, and the appropriate value of the parameter c (or c'). The value of the quantity $3\pi c/2\lambda\rho$ (or $3\pi c'/2\lambda\rho$) multiplied by the aerosol mass content M gives the extinction coefficient σ_e (or absorption coefficient σ_a). Also given in the table is the ratio of the absorption to the extinction coefficient σ_a/σ_e. The single-scatter albedo $w_o = 1 - \sigma_a/\sigma_e$.

	Extinction			Absorption			
λ(μm)	c	r_m(μm)	$\frac{3\pi c}{2\lambda\rho}$(m^{2}g^{-1})	c'	r_m(μm)	$\frac{3\pi c'}{2\lambda\rho}$(m^{2}g^{-1})	σ_a/σ_e
0.55	0.72	0.5	4.8 c				
1.06	0.69	1.0	2.6 c				
3.0	0.66	2.1	0.81a	0.43	1.3	0.52a	0.65
3.5	0.70	3.0	0.73b	0.20	3.1	0.20a	0.28
3.8	0.65	3.5	0.63c	0.16	3.0	0.16a	0.25
4.0	0.64	3.7	0.59c	0.17	3.3	0.16a	0.27
4.5	0.60	4.2	0.49c	0.19	3.2	0.16a	0.32
5.0	0.57	4.8	0.42c	0.22	3.3	0.16a	0.39
8.0	0.68	3.7	0.32a	0.58	2.3	0.27a	0.85
8.5	1.05	3.3	0.46a	0.84	2.2	0.37a	0.80
9.0	0.90	4.8	0.37a	0.65	2.8	0.27a	0.72
9.5	1.09	4.3	0.42a	0.84	2.5	0.33a	0.77
10.0	0.96	5.5	0.35b	0.53	3.8	0.19a	0.55
10.5	0.89	5.9	0.31c	0.44	5.0	0.16a	0.49
11.0	0.84	6.4	0.28a	0.58	4.0	0.20a	0.69
11.5	0.96	6.2	0.30b	0.58	4.4	0.18a	0.60
12.0	0.93	6.7	0.28b	0.54	4.5	0.16a	0.58

a - Error in $3\pi c/2\lambda\rho$ (or $3\pi c'/2\lambda\rho$) is estimated to be less than 30 percent.
b - Error in $3\pi c/2\lambda\rho$ (or $3\pi c'/2\lambda\rho$) is estimated to be less than 50 percent.
c - Error in $3\pi c/2\lambda\rho$ (or $3\pi c'/2\lambda\rho$) is estimated to be less than 100 percent.

TABLE A-13. 75 PERCENT SULFURIC ACID IN WATER
(density ρ = 1.669 g cm^{-3})

	Extinction			Absorption			
λ(μm)	c	r_m(μm)	$\frac{3\pi c}{2\lambda\rho}(m^2g^{-1})$	c'	r_m(μm)	$\frac{3\pi c'}{2\lambda\rho}(m^2g^{-1})$	σ_a/σ_e
0.55	0.78	0.50	4.0 c				
1.06	0.76	0.91	2.1 c				
3.0	0.55	2.7	0.52a	0.25	2.1	0.23a	0.45
3.5	0.68	2.5	0.55a	0.41	1.6	0.33a	0.60
3.8	0.73	2.7	0.54a	0.36	1.8	0.27a	0.50
4.0	0.72	2.9	0.51b	0.34	2.1	0.24a	0.48
4.5	0.68	3.5	0.42b	0.33	2.2	0.21a	0.50
5.0	0.67	3.9	0.38b	0.32	2.5	0.18a	0.48
8.0	1.27	2.0	0.44a	1.21	1.4	0.43a	0.98
8.5	1.80	2.0	0.60a	1.60	1.4	0.54a	0.90
9.0	1.49	3.0	0.46a	1.18	1.9	0.37a	0.80
9.5	1.75	2.8	0.53a	1.38	1.8	0.41a	0.78
10.0	1.51	3.9	0.42b	0.82	3.2	0.23a	0.55
10.5	1.32	4.5	0.36c	0.69	3.8	0.19a	0.51
11.0	1.33	4.3	0.34a	0.87	3.2	0.23a	0.67
11.5	1.63	4.2	0.40c	0.78	3.9	0.19a	0.48
12.0	1.48	5.0	0.35c	0.57	5.1	0.14a	0.39

a - Error in $3\pi c/2\lambda\rho$ (or $3\pi c'/2\lambda\rho$) is estimated to be less than 30 percent.
b - Error in $3\pi c/2\lambda\rho$ (or $3\pi c'/2\lambda\rho$) is estimated to be less than 50 percent.
c - Error in $3\pi c/2\lambda\rho$ (or $3\pi c'/2\lambda\rho$) is estimated to be less than 100 percent.

TABLE A-14

For phosphoric acid, HC, fuel oil, and FS smoke particles the backscatter gain G at wavelength $\lambda = 0.694\mu m$ (or $\lambda = 1.06\mu m$) can be approximated by linear functions of particle size parameter $G(\lambda, x) = c''(\lambda)\, x$ for $x \leq x_m$, or equivalently for $r \leq r_m$. This approximation leads to the aerosol backscatter coefficient σ_{bs} being proportional to the smoke mass content M according to equation (7). If particles in a polydispersion have radii $r \leq r_m$, from the table we can find the value of the quantity $3c''/8\lambda\rho$ which if multiplied by the aerosol mass content M gives the backscatter coefficient σ_{bs}.

Smoke Material		$\lambda(\mu m)$	c''	$r_m(\mu m)$	$\frac{3c''}{8\lambda\rho}$ $(m^2 g^{-1} sr^{-1})$
20%	H_3PO_4	0.694	0.078	1.3	0.038c
50%	H_3PO_4	0.694	0.13	1.4	0.052a
65%	H_3PO_4	0.694	0.18	1.4	0.067a
85%	H_3PO_4	0.694	0.26	1.3	0.082a
20%	$ZnCl_2$	0.694	0.079	1.2	0.036b
40%	$ZnCl_2$	0.694	0.12	1.4	0.046a
50%	$ZnCl_2$	0.694	0.16	1.4	0.055a
65%	$ZnCl_2$	0.694	0.23	1.3	0.068a
100%	Fuel oil	0.694	0.20	1.3	0.12 a
38%	H_2SO_4	0.694	0.090	1.3	0.038b
75%	H_2SO_4	0.694	0.15	1.5	0.048a
38%	H_2SO_4	1.06	0.082	2.0	0.023b
75%	H_2SO_4	1.06	0.14	2.7	0.030a

a - Error in $3c''/8\lambda\rho$ is estimated to be less than 30 percent.
b - Error in $3c''/8\lambda\rho$ is estimated to be less than 50 percent.
c - Error in $3c''/8\lambda\rho$ is estimated to be less than 100 percent.

TABLE A-15

Radius changes (r/r_o) of phosphoric acid droplets as a function of relative humidity f. The parameter r_o is the radius of a "dry" particle having density $\rho_o = 1.834$ g cm^{-3}. (After Hänel, private communication, 1978.)

r_o(cm):	10^{-6}	$3 \cdot 10^{-6}$	10^{-5}	$3 \cdot 10^{-5}$	10^{-4}	$3 \cdot 10^{-4}$	10^{-3}	$3 \cdot 10^{-3}$	10^{-2}
f					r/r_o				
0.2	1.075	1.078	1.078	1.078	1.078	1.078	1.078	1.078	1.078
0.4	1.213	1.236	1.236	1.236	1.236	1.236	1.236	1.236	1.236
0.6	1.327	1.346	1.352	1.353	1.354	1.354	1.354	1.354	1.354
0.7	1.396	1.425	1.436	1.440	1.441	1.441	1.441	1.441	1.441
0.8	1.489	1.535	1.555	1.561	1.563	1.564	1.564	1.564	1.564
0.9	1.652	1.752	1.795	1.810	1.816	1.817	1.817	1.818	1.818
0.95	1.800	2.002	2.093	2.122	2.133	2.136	2.136	2.137	2.137
0.975	1.936	2.259	2.461	2.528	2.553	2.560	2.563	2.564	2.564
0.99	2.053	2.614	3.091	3.287	3.362	3.385	3.392	3.394	3.396
0.995	2.102	2.853	3.676	4.076	4.240	4.289	4.307	4.312	4.314

TABLE A-16

Radius changes (r/r_o) of HC smoke droplets as a function of relative humidity f. The parameter r_o is the radius of a "dry" particle having density ρ_o = 2.91 g cm^{-3}. (After Hänel, private communication, 1978.)

r_o(cm):	10^{-6}	$3 \cdot 10^{-6}$	10^{-5}	$3 \cdot 10^{-5}$	10^{-4}	$3 \cdot 10^{-4}$	10^{-3}	$3 \cdot 10^{-3}$	10^{-2}
f					r/r_o				
0.2	1.207	1.210	1.210	1.211	1.211	1.211	1.211	1.211	1.211
0.4	1.354	1.382	1.394	1.398	1.399	1.400	1.400	1.400	1.400
0.6	1.519	1.555	1.568	1.572	1.573	1.573	1.573	1.573	1.573
0.7	1.624	1.669	1.682	1.685	1.687	1.687	1.687	1.687	1.687
0.8	1.740	1.794	1.818	1.825	1.827	1.828	1.828	1.828	1.828
0.85	1.817	1.896	1.928	1.938	1.944	1.945	1.945	1.945	1.945
0.9	1.930	2.076	2.134	2.151	2.157	2.159	2.160	2.160	2.160
0.95	2.162	2.452	2.593	2.638	2.653	2.658	2.660	2.660	2.660
0.975	2.386	2.953	3.246	3.340	3.372	3.382	3.385	3.386	3.386
0.99	2.651	3.677	4.279	4.493	4.573	4.597	4.605	4.608	4.608
0.995	2.791	4.170	5.182	5.583	5.739	5.784	5.801	5.806	5.807

TABLE A-17

Ratio of the extinction coefficient of phosphoric acid smoke to that for HC smoke as a function of relative humidity calculated according to equation (10).

λ(μm)	Relative Humidity			
	40%	60%	80%	95%
0.55	1.04	1.01	1.00	0.82
1.06	1.04	1.01	1.00	0.82
3.0	0.80	0.98	0.92	0.82
10.5	2.79	1.81	1.04	0.82
11.0	2.50	1.63	1.02	0.82
12.0	2.10	1.36	1.04	0.82

ELECTRO-OPTICS DIVISION DISTRIBUTION LIST

Commander
US Army Aviation Center
ATTN: ATZQ-D-MA
Fort Rucker, AL 36362

Commander
US Army Aviation School
Fort Rucker, AL 36362

Ballistic Missile Defense Advanced
Technology Center
ATTN: ATC-R
PO Box 1500
Huntsville, AL 35807

Lockheed-Huntsville Msl & Space Co.
ATTN: Dr. Lary W. Pinkley
PO Box 1103
West Station
Huntsville, AL 35807

Chief, Atmospheric Sciences Div
Code ES-81, NASA
Marshall Space Flight Center,
AL 35812

Project Manager
Patriot Missile Systems
ATTN: DRCPM-MD-T
Redstone Arsenal, AL 35809

Commander
US Army Missile R&D Command
ATTN: DRDMI-CGA (B. W. Fowler)
Redstone Arsenal, AL 35809

Redstone Scientific Information Center
ATTN: DRDMI-TBD
US Army Missile R&D Command
Redstone Arsenal, AL 35809

Commander
US Army Missile R&D Command
ATTN: DRDMI-TEM (R. Haraway)
Redstone Arsenal, AL 35809

Commander
US Army Missile R&D Command
ATTN: DRDMI-TRA (Dr. Essenwanger)
Redstone Arsenal, AL 35809

Commander
US Army Missiles and Munitions
Center & School
ATTN: ATSIC-CD
Redstone Arsenal, AL 35809

Commander
US Army Missile R&D Command
ATTN: DRDMI-REO (Dr. Maxwell Harper)
Redstone Arsenal, AL 35809

Commander
US Army Missile R&D Command
ATTN: DRDMI-RRE (Dr. Julius Lilly)
Redstone Arsenal, AL 35809

Commander
US Army Missile R&D Command
ATTN: DRDMI-TEO (Dr. Gene Widenhofer)
Redstone Arsenal, AL 35809

Commander
US Army Missile R&D Command
ATTN: DRDMI-HRO (Dr. D.B. Guenter)
Redstone Arsenal, AL 35809

Commander
US Army Missile R&D Command
ATTN: DRDMI-TDO (Dr. Hugh Anderson)
Redstone Arsenal, AL 35809

Commander
US Army Missile R&D Command
ATTN: DRDMI-YLA (Mr. W.S. Rich)
Redstone Arsenal, AL 35809

Commander
US Army Missile R&D Command
ATTN: DRDMI-TEG (Dr. George Emmons)
Redstone Arsenal, AL 35809

Commander
HQ, Fort Huachuca
ATTN: Tech Ref Div
Fort Huachuca, AZ 85613

Commander
US Army Intelligence Center & School
ATTN: ATSI-CD
Fort Huachuca, AZ 85613

Commander
US Army Intelligence Center & School
ATTN: ATSI-CD-CS (Mr. Jim Rustenbeck)
Fort Huachuca, AZ 85613

Commander
US Army Intelligence Center & School
ATTN: ATSI-CD-MD
Fort Huachuca, AZ 85613

Commander
US Army Communications Command
Fort Huachuca, AZ 85613

Commander
US Army Yuma Proving Ground
ATTN: Technical Library
Bldg 2100
Yuma, AZ 85364

Northrop Corporation
Electro-Mechanical Division
ATTN: Dr. R. D. Tooley
500 East Orangethorpe Ave
Anaheim, CA 92801

Naval Weapons Center
ATTN: Code 3173 (Dr. A. Shlanta)
China Lake, CA 93555

Hughes Helicopters
ATTN: Charles R. Hill
Centinela and Teale Streets
Culter City, CA 90230

Commander
US Army Combat Dev Evaluation Command
ATTN: ATEC-PL-M (Gary Love)
Fort Ord, CA 93941

SRI International
ATTN: Dr. Ed Uthe
333 Ravenswood Avenue
Menlo Park, CA 94025

SRI International
ATTN: J. E. Van der Laan
333 Ravenswood Avenue
Menlo Park, CA 94025

Sylvania Elec Sys Western Div
ATTN: Technical Reports Library
PO Box 205
Mountain View, CA 94040

Geophysics Officer
PMTC Code 3250
Pacific Missile Test Center
Point Mugu, CA 93042

Commander
Naval Ocean Systems Center
ATTN: Code 4473 (Tech Library)
San Diego, CA 92152

Commander
Naval Ocean Systems Center
ATTN: Code 532 (Dr. Juergen Richter)
San Diego, CA 92152

General Electric -TEMPO
ATTN: Dr. James Thompson
816 State Street
PO Drawer QQ
Santa Barbara, CA 93102

The RAND Corporation
ATTN: Ralph Huschke
1700 Main Street
Santa Monica, CA 90406

National Center for Atmos Research
NCAR Library
PO Box 3000
Boulder, CO 80307

Library-R-51-Tech Reports
NOAA/ERL
320 S. Broadway
Boulder, CO 80302

Wave Propagation Laboratory
NOAA/ERL
ATTN: Dr. Vernon Derr
Boulder, CO 80302

Particle Measuring Systems, Inc.
ATTN: Dr. Robert Knollenberg
1855 South 57th Court
Boulder, CO 80301

US Department of Commerce
Institute for Telecommunication Sciences
ATTN: Dr. H. J. Liebe
Boulder, CO 80303

HQDA (SAUS-OR/Hunter Woodall)
Rm 2E614, Pentagon
Washington, DC 20301

Dr. Herbert Fallin
ODUSA-OR
Rm 2E621, Pentagon
Washington, DC 20301

COL Elbert Friday
OUSDR&E
Rm 3D129, Pentagon
Washington, DC 20301

Defense Communications Agency
Technical Library Center
Code 205
Washington, DC 20305

Director
Defense Nuclear Agency
ATTN: Technical Library
Washington, DC 20305

Director
Defense Nuclear Agency
ATTN: RAAE (MAJ Ed Mueller)
Washington, DC 20305

Director
Defense Nuclear Agency
ATTN: SPAS (Mr. A.T. Hopkins)
Washington, DC 20305

Defense Intelligence Agency
ATTN: Scientific Advisory Committee
Washington, DC 20310

HQDA (DAMA-ARZ-D/Dr. Verderame)
Washington, DC 20310

HQDA (DAMI-ISP/Mr. Beck)
Washington, DC 20310

Department of the Army
Deputy Chief of Staff for
Operations and Plans
ATTN: DAMO-RQ
Washington, DC 20310

Department of the Army
Director of Telcommunications and
Command and Control
ATTN: DAMO-TCZ
Washington, DC 20310

Department of the Army
Deputy Chief of Staff for Research,
Development and Acquisition
ATTN: DAMA-AR
Washington, DC 20310

Department of the Army
Assistant Chief of Staff for Intelligence
ATTN: DAMI-TS
Washington, DC 20310

HQDA (DAEN-RDM/Dr. de Percin)
Forrestal Building
Washington, DC 20314

Director
Naval Research Laboratory
ATTN: Code 5530
Washington, DC 20375

Director
Naval Research Laboratory
ATTN: Code 2627
Washington, DC 20375

Director
Naval Research Laboratory
ATTN: Code 1409
(Dr. J. M. MacCallum)
Washington, DC 20375

Director
Naval Research Laboratory
ATTN: Code 5567
(Dr. James A. Dowling)
Washington, DC 20375

Director
Naval Research Laboratory
ATTN: Code 5567
(Dr. Steve Hanley)
Washington, DC 20375

Director
Naval Research Laboratory
ATTN: Code 8320
(Dr. L.H. Ruhnke)
Washington, DC 20375

The Library of Congress
ATTN: Exchange & Gift Div
Washington, DC 20540
2

Head, Atmos Rsch Section
Div Atmospheric Science
National Science Foundation
1800 G. Street, NW
Washington, DC 20550

ADTC/DLODL
Eglin AFB, FL 32542

Naval Training Equipment Center
ATTN: Technical Library
Orlando, FL 32813

Georgia Institute of Technology
ATTN: Dr. James Wiltse
Atlanta, GA 30332

Georgia Institute of Technology
ATTN: Dr. Robert McMillan
Atlanta, GA 30332

Georgia Institute of Technology
ATTN: Mr. James Gallagher
Atlanta, GA 30332

Commander
US Army Infantry Center
Fort Benning, GA 31805

Commander
US Army Infantry Center
ATTN: AT2B-CD
Fort Benning, GA 31805

US Army Signal School
ATTN: ATSN-CD
Fort Gordon, GA 30905

USAFETAC
Scott AFB, IL 62225

Commander
Air Weather Service
ATTN; DNPP (LTC Donald Hodges)
Scott AFB, IL 62269

Commander
US Army Combined Arms Center
ATTN: ATCA-CAA-? (Kent Pickett)
Fort Leavenworth, KS 66027

Commander
US Army Combined Arms Center
ATTN: ATCA-CS
Fort Leavenworth, KS 66027

Commander
US Army Combined Arms Center
ATTN: ATCA-CCC
Fort Leavenworth, KS 66027

Commander
US Army Combined Arms Center
ATTN: ATCA-CDC
Fort Leavenworth, KS 66027

Commander
US Army Combined Arms Center
ATTN: ATCA-CDE
Fort Leavenworth, KS 66027

Commander
US Army Combined Arms Center
ATTN: ATCA-CCM
Fort Leavenworth, KS 66027

Commander
US Army Armor Center
ATTN: ATZK-AE-TA
(Dr. Charles Leake)
Fort Knox, KY 40121

Commander
US Army Armor Center
ATTN: ATZK-CD
Fort Knox, KY 40121

Aerodyne Research Inc.
ATTN: Dr. John Ebersole
Bedford Research Park
Crosby Drive
Bedford, MA 01730

Commander
Air Force Geophysical Laboratory
ATTN: OPI (Dr. R.A. McClatchey)
Hanscom AFB, MA 01731

Commander
Air Force Geophysical Laboratory
ATTN: OPI (Dr. R. Fenn)
Hanscom AFB, MA 01731

Commander
US Army Ordnance Center and School
ATTN: ATSL-CD
Aberdeen Proving Ground, MD 21005

Commander
US Army Ordnance & Chemical Center
and School
ATTN: ATSL-CLC (Dr. Thomas Welch)
Aberdeen Proving Ground, MD 21005

Commander
US Army Ballistic Rsch Laboratory
ATTN: Dr. Robert Eichelberge
Aberdeen Proving Ground, MD 21005

Commander
US Army Ballistic Rsch Laboratory
ATTN: Mr. Alan Downs
Aberdeen Proving Ground, MD 21005

Commander
US Army Ballistic Rsch Laboratory
ATTN: DRDAR-BLB (Mr. Arthur LaGrange)
Aberdeen Proving Ground, MD 21005

Commander
US Army Ballistic Research Laboratory
ATTN: Mr. Richard McGee
Aberdeen Proving Ground, MD 21005

Project Manager
Smoke/Obscurants
ATTN: DRDPM-SMC (COL H. Shelton)
Aberdeen Proving Ground, MD 21005

Project Manager
Smoke/Obscurants
ATTN: DRDPM-SMC (Dr. T. Van de Wal Jr.)
Aberdeen Proving Ground, MD 21005

Project Manager
Smoke/Obscurants
ATTN: DRDPM-SMC (Mr. G. Bowman)
Aberdeen Proving Ground, MD 21005

Project Manager
Smoke/Obscurants
ATTN: DRDPM-SMC (Mr. J. Steedman)
Aberdeen Proving Ground, MD 21005

Commander
US Army Test & Evaluation Command
ATTN: DRSTE-AD-M (Mr. Warren M. Baily)
Aberdeen Proving Ground, MD 21005

Director
US Army Material Systems Analysis Activity
ATTN: DRXSY-LA (Mr. Paul Frossell)
Aberdeen Proving Ground, MD 21005

Director
US Army Material Systems Analysis Activity
ATTN: DRXSY-LA (Mr. Michael Starks)
Aberdeen Proving Ground, MD 21005

Director
US Army Material Systems Analysis Activity
ATTN: DRXSY-LA (Mr. William Smith)
Aberdeen Proving Ground, MD 21005

Director
US Army Material Systems Analysis Activity
ATTN: DRXSY-LA (Dr. Keats Pullen)
Aberdeen Proving Ground, MD 21005

Director
US Army Material Systems Analysis Activity
ATTN: DRXSY-GI (Mr. Sid Geraud)
Aberdeen Proving Ground, MD 21005

Director
US Army Armament R&D Command
Chemical Systems Laboratory
ATTN: DRDAR-CLB-PS (Dr. Ed Stuebing)
Aberdeen Proving Ground, MD 21010

Director
US Army Armament R&D Command
Chemical Systems Laboratory
ATTN: DRDAR-CLB-PS (Mr. Joseph Vervier)
Aberdeen Proving Ground, MD 21010

Director
US Army Armament R&D Command
Chemical Systems Laboratory
ATTN: DRDAR-CLY-A (Mr. Ron Pennsyle)
Aberdeen Proving Ground, MD 21010

Commander
Harry Diamond Laboratories
ATTN: Dr. William Carter
2800 Powder Mill Road
Adelphi, MD 20783

Commander
Harry Diamond Laboratories
ATTN: DELHD-RAC (Dr. R.G. Humphrey)
2800 Powder Mill Road
Adelphi, MD 20783

Commander
Harry Diamond Laboratories
ATTN: Dr. Ed Brown
2800 Powder Mill Road
Adelphi, MD 20783

Commander
Harry Diamond Laboratories
ATTN: Dr. Stan Kulpa
2800 Powder Mill Road
Adelphi, MD 20783

Commander
ERADCOM
ATTN: DRDEL-AP
2800 Powder Mill Road
Adelphi, MD 20783
2

Commander
ERADCOM
ATTN: DRDEL-CG/DRDEL-DC/DRDEL-CS
2800 Powder Mill Road
Adelphi, MD 20783

Commander
ERADCOM
ATTN: DRDEL-CT
2800 Powder Mill Road
Adelphi, MD 20783

Commander
ERADCOM
ATTN: DRDEL-EA
2800 Powder Mill Road
Adelphi, MD 20783

Commander
ERADCOM
ATTN: DRDEL-PA/DRDEL-ILS/DRDEL-E
2800 Powder Mill Road
Adelphi, MD 20783

Commander
ERADCOM
ATTN: DRDEL-PAO (S. Kimmel)
2800 Powder Mill Road
Adelphi, MD 20783

Commander
ERADCOM
ATTN: DRDEL-PAO (Paul Case)
2800 Powder Mill Road
Adelphi, MD 20783

Commander
HQ, AFSC/DLCAA
ATTN: LTC Glen Warner
Andrews AFB, MD 20334

AFSC
ATTN: WER (Mr. Richard F. Picanso)
Andrews AFB, MD 20334

Commander
Concepts Analysis Agency
ATTN: MOCA-SMC (Hal E. Hock)
8120 Woodmont Ave
Bethesda, MD 20014

Martin Marietta Laboratories
ATTN: Jar Mo Chen
1450 South Rolling Road
Baltimore, MD 21227

Commander
US Army Intelligence Agency
Fort George G. Meade, MD 20755

Director
National Security Agency
ATTN: R52/Woods
Fort George G. Meade, MD 20755

Chief
Intelligence Materiel Dev & Support Ofc
ATTN: DELEW-WL-I
Bldg 4554
Fort George G. Meade, MD 20755

Acquisitions Section, IRDB-D823
Library & Info Service Div, NOAA
6009 Executive Blvd
Rockville, MD 20852

Naval Surface Weapons Center
ATTN: Code WR42 (Dr. Barry Katz)
White Oak Library
Silver Spring, MD 20910

The Environmental Research
Institute of MI
ATTN: IRIA Library
PO Box 8618
Ann Arbor, MI 48107

Science Applications Inc.
ATTN: Dr. Robert E. Meredith
15 Research Drive
PO Box 7329
Ann Arbor, MI 48107

Science Applications Inc.
ATTN: Dr. Robert E. Turner
15 Research Drive
PO Box 7329
Ann Arbor, MI 48107

Commander
US Army Tank-Automative R&D Command
Warren, MI 48090

Dr. A. D. Belmont
Research Division
PO Box 1249
Control Data Corp
Minneapolis, MN 55440

Commander
US Army Aviation Systems Command
St. Louis, MO 63166

Director
Naval Oceanography & Meteorology
NSTL Station
Bay St Louis, MS 39529

Director
US Army Engr Waterways Experiment Sta
ATTN: Library
PO Box 631
Vicksburg, MS 39180

Director
US Army Engr Waterways Experiment Sta
ATTN: WESFT (Dr. Bob Penn)
PO Box 631
Vicksburg, MS 39180

Director
US Army Engr Waterways Experiment Sta
ATTN: WESFT (Mr. Jerry Lundien)
PO Box 631
Vicksburg, MS 39180

US Army Research Office
ATTN: DRXRO-PP
PO Box 12211
Research Triangle Park, NC 27709

US Army Research Office
ATTN: DRXRO-GS (Dr. Arthur V. Dodd)
PO Box 12211
Research Triangle Park, NC 27709

Commander
US Army Cold Regions Rsch & Engr Lab
ATTN: Mr. Roger Berger
Hanover, NH 03755

Commander
US Army Cold Regions Rsch & Engr Lab
ATTN: Mr. George Aitken
Hanover, NH 03755

Commander
US Army Cold Regions Rsch & Engr Lab
ATTN: CRREL-RD (Dr. K.F. Sterrett)
Hanover, NH 03755

Commander
US Army Armament R&D Command
ATTN: DRDAR-TSS (Bldg 59)
Dover, NJ 07801

Commander
US Army Armament R&D Command
ATTN: DRDAR-AC (J. Greenfield)
Dover, NJ 07801

Project Manager
Cannon Artillery Weapons Systems
ATTN: DRCPM-CAWS
Dover, NJ 07801

Project Manager
Cannon Artillery Weapons Systems
ATTN: DRCPM-CAWS-GP (G.H. Waldron)
Dover, NJ 07801

Commander
HQ, US Army Avionics R&D Activity
ATTN: DAVAA-O
Fort Monmouth, NJ 07703

Commander/Director
US Army Combat Surveillance & Target
Acquisition Laboratory
ATTN: DELCS-D
Fort Monmouth, NJ 07703

Director
US Army Electronics Technology &
Devices Laboratory
ATTN: DELET-D
Fort Monmouth, NJ 07703

Commander
US Army Electronic Warfare Laboratory
ATTN: DELEW-D (Mr. George Haber)
Fort Monmouth, NJ 07703

Commander
US Army Night Vision &
Electro-Optics Laboratory
ATTN: DELNV-L (Dr. Rudolf Buser)
Fort Monmouth, NJ 07703

Commander
US Army Night Vision &
Electro-Optics Laboratory
ATTN: DELNV-L (Dr. Robert Rodhe)
Fort Monmouth, NJ 07703

Commander
ERADCOM Technical Support Activity
ATTN: DELSD-L
Fort Monmouth, NJ 07703

Project Manager, FIREFINDER
ATTN: DRCPM-FF
Fort Monmouth, NJ 07703

Project Manager, REMBASS
ATTN: DRCPM-RBS
Fort Monmouth, NJ 07703

Commander
US Army Satellite Comm Agency
ATTN: DRCPM-SC-3
Fort Monmouth, NJ 07703

Commander
ERADCOM Scientific Advisor
ATTN: DRDEL-SA
Fort Monmouth, NJ 07703

Project Manager
Army Tactical Data Systems
ATTN: DRCPM-TDS
Fort Monmouth, NJ 07703

6585 TG/WE
Holloman AFB, NM 88330

AFWL/WE
Kirtland, AFB, NM 87117

AFWL/Technical Library (SUL)
Kirtland AFB, NM 87117

Commander
US Army Test & Evaluation Command
ATTN: STEWS-AD-L
White Sands Missile Range, NM 88002

Chief
US Army Electronics R&D Command
Office of Missile Electronic Warfare
ATTN: DELEW-M-STE (Dr. Steven Kovel)
White Sands Missile Range, NM 88002

US Army Office of the Test Director
Joint Services EO GW CM Test Program
ATTN: DRXDE-TD (Mr. Weldon Findley)
White Sands Missile Range, NM 88002

Commander
TRASANA
ATTN: ATAA-D (Dr. Wilbur Payne)
White Sands Missile Range, NM 88002

Commander
TRASANA
ATTN: ATAA-TDB (Louis Dominquez)
White Sands Missile Range, NM 88002

Commander
TRASANA
ATTN: ATAA-PL (Dolores Anguiano)
White Sands Missile Range, NM 88002

Commander
TRASANA
ATTN: ATAA-TOP (Roger Willis)
White Sands Missile Range, NM 88002

Commander
TRASANA
ATTN: ATAA-TGC (Dr. Alfonso Diaz)
White Sands Missile Range, NM 88002

Commander
TRASANA
ATTN: ATAA-TGA (Mr. Edward Henry)
White Sands Missile Range, NM 88002

Grumman Aerospace Corporation
Research Dept - MS A08-35
ATTN: John E. A. Selby
Bethpage, NY 11714

Rome Air Development Center
ATTN: Documents Library
TSLD (Bette Smith)
Griffiss AFB, NY 13441

Commander
US Army Tropic Test Center
ATTN: STETC-TD (Info Center)
APO New York 09827

Commander
US Army R&D Coordinator
US Embassy, Bonn, Box 165
APO New York 09080

HQ
USAREUR & Seventh Army
APO New York, NY 09403

Air Force Avionics Laboratory
ATTN: AFAL/RWI-3 (Cpt James Pryce)
Wright-Patterson AFB, OH 45433

Air Force Air Systems Laboratory
ATTN: AFAL/RWI-e (Dr. George Mavko)
Wright-Patterson AFB, OH 45433

Commandant
US Army Field Artillery School
ATTN: ATSF-CD-R (Mr. Farmer)
Fort Sill, OK 73503

Commandant
US Army Field Artillery School
ATTN: ATSF-CF-R
Fort Sill, OK 73503

Director CFD
US Army Field Artillery School
ATTN: Met Division
Fort Sill, OK 73503

Commandant
US Army Field Artillery School
ATTN: Morris Swett Library
Fort Sill, OK 73503

Commander
US Army Combined Arms Center
ATTN: ATCA-CAT-V (R. DeKinder, Jr.)
Fort Sill, OK 73503

US Army Field Artillery School
ATTN: ATSF-CD
Fort Sill, OK 73503

Commander
273rd Transportation Company
(Heavy Helicopter)
W44CCQ
ATTN: CW4 J. Kard
Fort Sill, OK 73503

Commander
Naval Air Development Center
ATTN: Code 202 (Mr. Thomas Shopple)
Warminster, PA 18974

University of Texas at El Paso
Electrical Engineering Department
ATTN: Dr. Joseph H. Pierluissi
El Paso, TX 79968

US Army Air Defense School
ATTN: ATSA-CD
Fort Bliss, TX 79916

Commander
3rd Armored Cavalry Regiment
ATTN: AFVF-SO
Fort Bliss, TX 79916

Commander
TRADOC Combined Arms Test Activity
ATTN: ATCAT-OP-Q (Wayland Smith)
Fort Hood, TX 76544

Commander
TRADOC Combined Arms Test Activity
ATTN: Technical Library
Fort Hood, TX 76544

Commander
TRADOC Combined Arms Test Activity
ATTN: ATCAT-SCI (Darrell Collin)
Fort Hood, TX 76544

MAJ Joseph Caruso
HQ, TRADOC Combined Arms Test Activity
ATTN: ATCAT-CA
Fort Hood, TX 76544

Commandant
US Army Air Defense School
ATTN: Mr. Blanchett
Fort Bliss, TX 79916

Commander
US Army Dugway Proving Ground
ATTN: STEDP-MT-DA-L
Dugway, UT 84022

Commander
US Army Dugway Proving Ground
ATTN: STEDP-MT-DA-S (John Treatheway)
Dugway, UT 84022

Commander
US Army Dugway Proving Ground
ATTN: STEDP-MT-DA-M (Paul Carlson)
Dugway, UT 84022

Commander
US Army Dugway Proving Ground
ATTN: STEDP-MT-DA-T (William Peterson)
Dugway, UT 84022

Defense Documentation Center
ATTN: DDC-TCA
Cameron Station Bldg 5
Alexandria, VA 22314
12

Ballistic Missile Defense Program Office
ATTN: DACS-BMT
5001 Eisenhower Avenue
Alexandria, VA 22333

Commander
US Army Materiel Dev & Readiness Command
ATTN: DRCLDC (Mr. James Bender)
5001 Eisenhower Ave
Alexandria, VA 22333

Commander
US Army Materiel Dev & Readiness Command
ATTN: DRCBSI
5001 Eisenhower Ave
Alexandria, VA 22333

Institute for Defense Analysis
ATTN: Mr. Lucian Biberman
Arlington, VA 22202

Institute for Defense Analysis
ATTN: Dr. Robert Roberts
Arlington, VA 22202

Director
ARPA
1400 Wilson Blvd
Arlington, VA 22209

Defense Advanced Rsch Projects Agency
ATTN: Steve Zakanyez
1400 Wilson Blvd
Arlington, VA 22209

Defense Advanced Rsch Projects Agency
ATTN: Dr. Carl Thomas
1400 Wilson Blvd
Arlington, VA 22209

Defense Advanced Rsch Projects Agency
ATTN: Dr. James Tegnelia
1400 Wilson Blvd
Arlington, VA 22209

Commander
US Army Security Agency
ATTN: IARD-MF
Arlington Hall Station
Arlington, VA 22212

USA Intelligence & Security Command
ATTN: E. A. Speakman,
Science Advisor
Arlington Hall Station
Arlington, VA 22212

Commander
US Army Foreign Sci & Tech Center
ATTN: DRXST-IS1
220 7th Street, NE
Charlottesville, VA 22901

Commander
US Army Foreign Sci & Tech Center
ATTN: Dr. Orville Harris
220 7th Street, NE
Charlottesville, VA 22901

Commander
US Army Foreign Sci & Tech Center
ATTN: Dr. Bertram Smith
220 7th Street, NE
Charlottesville, VA 22901

Naval Surface Weapons Center
ATTN: Code G65
Dahlgren, VA 22448

Commander
Operational Test & Evaluation Agency
Columbia Pike Bldg
5600 Columbia Pike
Falls Church, VA 22041

Commander
US Army Night Vision
& Electro-Optics Lab
ATTN: DELNV-D (Mr. John Johnson)
Fort Belvoir, VA 22060

Commander
US Army Night Vision
& Electro-Optics Lab
ATTN: DELNV-VI (Mr. J.R. Moulton)
Fort Belvoir, VA 22060

Commander
US Army Night Vision
& Electro-Optics Lab
ATTN: DELNV-VI (Luanne Overt)
Fort Belvoir, VA 22060

Commander
US Army Night Vision
& Electro-Optics Lab
ATTN: DELNV-VI (Tom Cassidy)
Fort Belvoir, VA 22060

Commander
US Army Night Vision
& Electro-Optics Lab
ATTN: DELNV-VI (Richard Bergemann)
Fort Belvoir, VA 22060

Commander
US Army Night Vision
& Electro-Optics Lab
ATTN: DELNV-VI (Dr. John Ratches)
Fort Belvoir, VA 22060

Commander
US Army Night Vision
& Electro-Optics Lab
ATTN: DELNV-FIR (Fred Petito)
Fort Belvoir, VA 22060

Commander
US Army Engineering Topographic Lab
ATTN: ETL-TD-MB
Fort Belvoir, VA 22060

US Army Engineer School
ATTN: ATSE-CD
Fort Belvoir, VA 22060

Commandant
US Army Engineering Center & School
Directorate of Combat Developments
Fort Belvoir, VA 22060

Commander
US Army Mobility Equip R&D Command
ATTN: DRDME-RT (Mr. Fred Kezer)
Fort Belvoir, VA 22060

Director
Applied Technology Laboratory
ATTN: DAVDL-EU-TSD (Tech Library)
Fort Eustis, VA 23604

Department of the Air Force
OL-C, 5WW
Fort Monroe, VA 23651

Commander
HQ, TRADOC
ATTN: ATCD-PM
Fort Monroe, VA 23651

Commander
US Army Training & Doctrine Command
Fort Monroe, VA 23651

Commander
US Army Training & Doctrine Command
ATTN: ATCD-IE-R (Mr. Dave Ingram)
Fort Monroe, VA 23651

Commander
US Army Training & Doctrine Command
ATTN: ATCD-STE
Fort Monroe, VA 23651

Commander
US Army Training & Doctrine Command
ATTN: ATCD-CF (Chris O'Conner)
Fort Monroe, VA 23651

Commander
US Army Training & Doctrine Command
ATTN: ATCD-AN-TD (Seymour Goldbert)
Fort Monroe, VA 23651

Commander
US Army Training & Doctrine Command
ATTN: ATCD-TA (M. P. Pastel)
Fort Monroe, VA 23651

Commander
US Army Training & Doctrine Command
ATTN: Tech Library
Fort Monroe, VA 23651

Department of the Air Force
5WW/DN
Langley AFB, VA 23665

Commander
US Army INSCOM/QRC
6845 Elm Street - S407
McLean, VA 22101

MITRE Corporation
ATTN: Robert Finkelstein
1820 Dolley Madison Blvd
McLean, VA 22101

Science Applications, Inc.
8400 Westpark Drive
ATTN: Dr. John E. Cockayne
McLean, VA 22101

Director
Development Center MCDEC
ATTN: Firepower Division
Quantico, VA 22134

US Army Nuclear & Chemical Agency
ATTN: MONA-WE (Dr. Jack Berberet)
7500 Backlick Road
Springfield, VA 22150

Director
US Army Signals Warfare Laboratory
ATTN: DELSW-OS (Dr. R. Burkhardt)
Vint Hill Farms Station
Warrenton, VA 22186

Commander
US Army Cold Regions Test Center
ATTN: STECR-OP-PM
APO Seattle, WA 98733

Effects Technology Inc.
ATTN: Jack Carlyle
5383 Hollister Avenue
Santa Barbara, CA 93111

Raytheon Company
Electro-Optics Department
ATTN: Dr. Charles M. Sonnenschein
Boston Post Road
Wayland, MA 01778

Norden Systems
ATTN: Estelle Thurman, Librarian
Norwalk, CT 06856

MIT Lincoln Laboratory
ATTN: Dr. T. Goblick, D-447
PO Box 73
Lexington, MA 02173

Commander/Director
US Army Combat Surveillance & Target
Acquisition Laboratory
ATTN: DELCS-R (Mr. David Longinotti)
Fort Monmouth, NJ 07703

General Research Corporation
ATTN: Dr. Ralph Zirkind
7655 Old Springhouse Road
McLean, VA 22101

Commander
MIRADCOM
ATTN: DRDMI-TE (Mr. W. J. Lindberg)
Huntsville, AL 35807

Teledyne Brown Engineering
ATTN: Bruce Tully, Mail Stop 19
Cummings Research Park
Huntsville, AL 35807

Applied Physics Laboratory
John Hopkins University
ATTN: Dr. Michael Lun
John Hopkins Road
Laurell, MD 20810

ATMOSPHERIC SCIENCES RESEARCH PAPERS

1. Lindberg, J.D., "An Improvement to a Method for Measuring the Absorption Coefficient of Atmospheric Dust and other Strongly Absorbing Powders, " ECOM-5565, July 1975.
2. Avara, Elton, P., "Mesoscale Wind Shears Derived from Thermal Winds," ECOM-5566, July 1975.
3. Gomez, Richard B., and Joseph H. Pierluissi, "Incomplete Gamma Function Approximation for King's Strong-Line Transmittance Model," ECOM-5567, July 1975.
4. Blanco, A.J., and B.F. Engebos, "Ballistic Wind Weighting Functions for Tank Projectiles," ECOM-5568, August 1975.
5. Taylor, Fredrick J., Jack Smith, and Thomas H. Pries, "Crosswind Measurements through Pattern Recognition Techniques," ECOM-5569, July 1975.
6. Walters, D.L., "Crosswind Weighting Functions for Direct-Fire Projectiles," ECOM-5570, August 1975.
7. Duncan, Louis D., "An Improved Algorithm for the Iterated Minimal Information Solution for Remote Sounding of Temperature," ECOM-5571, August 1975.
8. Robbiani, Raymond L., "Tactical Field Demonstration of Mobile Weather Radar Set AN/TPS-41 at Fort Rucker, Alabama," ECOM-5572, August 1975.
9. Miers, B., G. Blackman, D. Langer, and N. Lorimier, "Analysis of SMS/GOES Film Data," ECOM-5573, September 1975.
10. Manquero, Carlos, Louis Duncan, and Rufus Bruce, "An Indication from Satellite Measurements of Atmospheric CO2 Variability," ECOM-5574, September 1975.
11. Petracca, Carmine, and James D. Lindberg, "Installation and Operation of an Atmospheric Particulate Collector," ECOM-5575, September 1975.
12. Avara, Elton P., and George Alexander, "Empirical Investigation of Three Iterative Methods for Inverting the Radiative Transfer Equation," ECOM-5576, October 1975.
13. Alexander, George D., "A Digital Data Acquisition Interface for the SMS Direct Readout Ground Station — Concept and Preliminary Design," ECOM-5577, October 1975.
14. Cantor, Israel, "Enhancement of Point Source Thermal Radiation Under Clouds in a Nonattenuating Medium," ECOM-5578, October 1975.
15. Norton, Colburn, and Glenn Hoidale, "The Diurnal Variation of Mixing Height by Month over White Sands Missile Range, N.M," ECOM-5579, November 1975.
16. Avara, Elton P., "On the Spectrum Analysis of Binary Data," ECOM-5580, November 1975.
17. Taylor, Fredrick J., Thomas H. Pries, and Chao-Huan Huang, "Optimal Wind Velocity Estimation," ECOM-5581, December 1975.
18. Avara, Elton P., "Some Effects of Autocorrelated and Cross-Correlated Noise on the Analysis of Variance, " ECOM-5582, December 1975.
19. Gillespie, Patti S., R.L. Armstrong, and Kenneth O. White, "The Spectral Characteristics and Atmospheric CO2 Absorption of the Ho^{+3}:YLF Laser at 2.05μm," ECOM-5583, December 1975.
20. Novlan, David J. "An Empirical Method of Forecasting Thunderstorms for the White Sands Missile Range," ECOM-5584, February 1976.
21. Avara, Elton P., "Randomization Effects in Hypothesis Testing with Autocorrelated Noise," ECOM-5585, February 1976.
22. Watkins, Wendell R., "Improvements in Long Path Absorption Cell Measurement," ECOM-5586, March 1976.
23. Thomas, Joe, George D. Alexander, and Marvin Dubbin, "SATTEL — An Army Dedicated Meteorological Telemetry System," ECOM-5587, March 1976.
24. Kennedy, Bruce W., and Delbert Bynum, "Army User Test Program for the RDT&E-XM-75 Meteorological Rocket," ECOM-5588, April 1976.

25. Barnett, Kenneth M., "A Description of the Artillery Meteorological Comparisons at White Sands Missle Range, October 1974 - December 1974 ('PASS' - Prototype Artillery [Meteorological] Subsystem)," ECOM-5589, April 1976.
26. Miller, Walter B., "Preliminary Analysis of Fall-of-Shot From Project 'PASS'," ECOM-5590, April 1976.
27. Avara, Elton P., "Error Analysis of Minimum Information and Smith's Direct Methods for Inverting the Radiative Transfer Equation," ECOM-5591, April 1976.
28. Yee, Young P., James D. Horn, and George Alexander, "Synoptic Thermal Wind Calculations from Radiosonde Observations Over the Southwestern United States," ECOM-5592, May 1976.
29. Duncan, Louis D., and Mary Ann Seagraves, "Applications of Empirical Corrections to NOAA-4 VTPR Observations," ECOM-5593, May 1976.
30. Miers, Bruce T., and Steve Weaver, "Applications of Meterological Satellite Data to Weather Sensitive Army Operations,"ECOM-5594, May 1976.
31. Sharenow, Moses, "Redesign and Improvement of Balloon ML-566," ECOM-5595, June, 1976.
32. Hansen, Frank V., "The Depth of the Surface Boundary Layer," ECOM-5596, June 1976.
33. Pinnick, R.G., and E.B. Stenmark, "Response Calculations for a Commercial Light-Scattering Aerosol Counter," ECOM-5597, July 1976.
34. Mason, J., and G.B. Hoidale, "Visibility as an Estimator of Infrared Transmittance," ECOM-5598, July 1976.
35. Bruce, Rufus E., Louis D. Duncan, and Joseph H. Pierluissi, "Experimental Study of the Relationship Between Radiosonde Temperatures and Radiometric-Area Temperatures," ECOM-5599, August 1976.
36. Duncan, Louis D., "Stratospheric Wind Shear Computed from Satellite Thermal Sounder Measurements," ECOM-5800, September 1976.
37. Taylor, F., P. Mohan, P. Joseph and T. Pries, "An All Digital Automated Wind Measurement System," ECOM-5801, September 1976.
38. Bruce, Charles, "Development of Spectrophones for CW and Pulsed Radiation Sources," ECOM-5802, September 1976.
39. Duncan, Louis D., and Mary Ann Seagraves,"Another Method for Estimating Clear Column Radiances," ECOM-5803, October 1976.
40. Blanco, Abel J., and Larry E. Taylor, "Artillery Meteorological Analysis of Project Pass," ECOM-5804, October 1976.
41. Miller, Walter, and Bernard Engebos," A Mathematical Structure for Refinement of Sound Ranging Estimates," ECOM-5805, November, 1976.
42. Gillespie, James B., and James D. Lindberg, "A Method to Obtain Diffuse Reflectance Measurements from 1.0 to 3.0 μm Using a Cary 17I Spectrophotometer," ECOM-5806, November 1976.
43. Rubio, Roberto, and Robert O. Olsen,"A Study of the Effects of Temperature Variations on Radio Wave Absorption,"ECOM-5807, November 1976.
44. Ballard, Harold N., "Temperature Measurements in the Stratosphere from Balloon-Borne Instrument Platforms, 1968-1975," ECOM-5808, December 1976.
45. Monahan, H.H., "An Approach to the Short-Range Prediction of Early Morning Radiation Fog," ECOM-5809, January 1977.
46. Engebos, Bernard Francis, "Introduction to Multiple State Multiple Action Decision Theory and Its Relation to Mixing Structures," ECOM-5810, January 1977.
47. Low, Richard D.H.,"Effects of Cloud Particles on Remote Sensing from Space in the 10-Micrometer Infrared Region," ECOM-5811, January 1977.
48. Bonner, Robert S., and R. Newton, "Application of the AN/GVS-5 Laser Rangefinder to Cloud Base Height Measurements," ECOM-5812, February 1977.
49. Rubio, Roberto, "Lidar Detection of Subvisible Reentry Vehicle Erosive Atmospheric Material," ECOM-5813, March 1977.
50. Low, Richard D.H., and J.D. Horn, "Mesoscale Determination of Cloud-Top Height: Problems and Solutions," ECOM-5814, March 1977.

51. Duncan, Louis D., and Mary Ann Seagraves, "Evaluation of the NOAA-4 VTPR Thermal Winds for Nuclear Fallout Predictions," ECOM-5815, March 1977.
52. Randhawa, Jagir S., M. Izquierdo, Carlos McDonald and Zvi Salpeter, "Stratospheric Ozone Density as Measured by a Chemiluminescent Sensor During the Stratcom VI-A Flight," ECOM-5816, April 1977.
53. Rubio, Roberto, and Mike Izquierdo, "Measurements of Net Atmospheric Irradiance in the 0.7- to 2.8-Micrometer Infrared Region," ECOM-5817, May 1977.
54. Ballard, Harold N., Jose M. Serna, and Frank P. Hudson Consultant for Chemical Kinetics, "Calculation of Selected Atmospheric Composition Parameters for the Mid-Latitude, September Stratosphere," ECOM-5818, May 1977.
55. Mitchell, J.D., R.S. Sagar, and R.O. Olsen, "Positive Ions in the Middle Atmosphere During Sunrise Conditions," ECOM-5819, May 1977.
56. White, Kenneth O., Wendell R. Watkins, Stuart A. Schleusener, and Ronald L. Johnson, "Solid-State Laser Wavelength Identification Using a Reference Absorber," ECOM-5820, June 1977.
57. Watkins, Wendell R., and Richard G. Dixon, "Automation of Long-Path Absorption Cell Measurements," ECOM-5821, June 1977.
58. Taylor, S.E., J.M. Davis, and J.B. Mason, "Analysis of Observed Soil Skin Moisture Effects on Reflectance," ECOM-5822, June 1977.
59. Duncan, Louis D. and Mary Ann Seagraves, "Fallout Predictions Computed from Satellite Derived Winds," ECOM-5823. June 1977.
60. Snider, D.E., D.G. Murcray, F.H. Murcray, and W.J. Williams, "Investigation of High-Altitude Enhanced Infrared Backround Emissions" (U), SECRET, ECOM-5824, June 1977.
61. Dubbin, Marvin H. and Dennis Hall, "Synchronous Meteorlogical Satellite Direct Readout Ground System Digital Video Electronics," ECOM-5825, June 1977.
62. Miller, W., and B. Engebos, "A Preliminary Analysis of Two Sound Ranging Algorithms," ECOM-5826, July 1977.
63. Kennedy, Bruce W., and James K. Luers, "Ballistic Sphere Techniques for Measuring Atomspheric Parameters," ECOM-5827, July 1977.
64. Duncan, Louis D., "Zenith Angle Variation of Satellite Thermal Sounder Measurements," ECOM-5828, August 1977.
65. Hansen, Frank V., "The Critical Richardson Number," ECOM-5829, September 1977.
66. Ballard, Harold N., and Frank P. Hudson (Compilers), "Stratospheric Composition Balloon-Borne Experiment," ECOM-5830, October 1977.
67. Barr, William C., and Arnold C. Peterson, "Wind Measuring Accuracy Test of Meteorological Systems," ECOM-5831, November 1977.
68. Ethridge, G.A. and F.V. Hansen, "Atmospheric Diffusion: Similarity Theory and Empirical Derivations for Use in Boundary Layer Diffusion Problems," ECOM-5832, November 1977.
69. Low, Richard D.H., "The Internal Cloud Radiation Field and a Technique for Determining Cloud Blackness," ECOM-5833, December 1977.
70. Watkins, Wendell R., Kenneth O. White, Charles W. Bruce, Donald L. Walters, and James D. Lindberg, "Measurements Required for Prediction of High Energy Laser Transmission," ECOM-5834, December 1977.
71. Rubio, Robert, "Investigation of Abrupt Decreases in Atmospherically Backscattered Laser Energy," ECOM-5835. December 1977.
72. Monahan, H.H. and R.M. Cionco, "An Interpretative Review of Existing Capabilities for Measuring and Forecasting Selected Weather Variables (Emphasizing Remote Means)," ASL-TR-0001, January 1978.
73. Heaps, Melvin G., "The 1979 Solar Eclipse and Validation of D-Region Models," ASL-TR-0002. March 1978.

74. Jennings, S.G., and J.B. Gillespie, "M.I.E. Theory Sensitivity Studies - The Effects of Aerosol Complex Refractive Index and Size Distribution Variations on Extinction and Absorption Coefficients Part II: Analysis of the Computational Results," ASL-TR-0003, March 1978.
75. White, Kenneth O. et al, "Water Vapor Continuum Absorption in the 3.5μm to 4.0μm Region," ASL-TR-0004, March 1978.
76. Olsen, Robert O., and Bruce W. Kennedy, "ABRES Pretest Atmospheric Measurements," ASL-TR-0005, April 1978.
77. Ballard, Harold N., Jose M. Serna, and Frank P. Hudson, "Calculation of Atmospheric Composition in the High Latitude September Stratosphere," ASL-TR-0006, May 1978.
78. Watkins, Wendell R. et al, "Water Vapor Absorption Coefficients at HF Laser Wavelengths," ASL-TR-0007, May 1978.
79. Hansen, Frank V., "The Growth and Prediction of Nocturnal Inversions," ASL-TR-0008, May 1978.
80. Samuel, Christine, Charles Bruce, and Ralph Brewer, "Spectrophone Analysis of Gas Samples Obtained at Field Site," ASL-TR-0009, June 1978.
81. Pinnick, R.G. et al., "Vertical Structure in Atmospheric Fog and Haze and its Effects on IR Extinction," ASL-TR-0010, July 1978.
82. Low, Richard D.H., Louis D. Duncan, and Richard B. Gomez, "The Microphysical Basis of Fog Optical Characterization," ASL-TR-0011, August 1978.
83. Heaps, Melvin G., "The Effect of a Solar Proton Event on the Minor Neutral Constituents of the Summer Polar Mesosphere," ASL-TR-0012, August 1978.
84. Mason, James B., "Light Attenuation in Falling Snow," ASL-TR-0013, August 1978.
85. Blanco, Abel J., "Long-Range Artillery Sound Ranging: "PASS" Meteorological Application," ASL-TR-0014, September 1978.
86. Heaps, M.G., and F.E. Niles, "Modeling the Ion Chemistry of the D-Region: A case Study Based Upon the 1966 Total Solar Eclipse," ASL-TR-0015, September 1978.
87. Jennings, S.G., and R.G. Pinnick, "Effects of Particulate Complex Refractive Index and Particle Size Distribution Variations on Atmospheric Extinction and Absorption for Visible Through Middle-Infrared Wavelengths," ASL-TR-0016, September 1978.
88. Watkins, Wendell R., Kenneth O. White, Lanny R. Bower, and Brian Z. Sojka, " Pressure Dependence of the Water Vapor Continuum Absorption in the 3.5- to 4.0-Micrometer Region," ASL-TR-0017, September 1978.
89. Miller, W.B., and B.F. Engebos, "Behavior of Four Sound Ranging Techniques in an Idealized Physical Enviroment," ASL-TR-0018, September 1978.
90. Gomez, Richard G., "Effectiveness Studies of the CBU-88/B Bomb, Cluster, Smoke Weapon" (U), CONFIDENTIAL ASL-TR-0019, September 1978.
91. Miller, August, Richard C. Shirkey, and Mary Ann Seagraves, "Calculation of Thermal Emission from Aerosols Using the Doubling Technique," ASL-TR-0020, November, 1978.
92. Lindberg, James D. et al., "Measured Effects of Battlefield Dust and Smoke on Visible, Infrared, and Millimeter Wavelengths Propagation: A Preliminary Report on Dusty Infrared Test-I (DIRT-I)," ASL-TR-0021, January 1979.
93. Kennedy, Bruce W., Arthur Kinghorn, and B.R. Hixon, "Engineering Flight Tests of Range Meteorological Sounding System Radiosonde," ASL-TR-0022, February 1979.
94. Rubio, Roberto, and Don Hoock, "Microwave Effective Earth Radius Factor Variability at Wiesbaden and Balbas," ASL-TR-0023, February 1979.
95. Low, Richard D.H., "A Theoretical Investigation of Cloud/Fog Optical Properties and Their Spectral Correlations," ASL-TR-0024, February 1979.

96. Pinnick, R.G., and H.J. Auvermann, "Response Characteristics of Knollenberg Light-Scattering Aerosol Counters," ASL-TR-0025, February 1979.
97. Heaps, Melvin G., Robert O. Olsen, and Warren W. Berning, "Solar Eclipse 1979, Atmospheric Sciences Laboratory Program Overview," ASL-TR-0026 February 1979.
98. Blanco, Abel J., "Long-Range Artillery Sound Ranging: 'PASS' GR-8 Sound Ranging Data," ASL-TR-0027, March 1979.
99. Kennedy, Bruce W., and Jose M. Serna, "Meteorological Rocket Network System Reliability," ASL-TR-0028, March 1979.
100. Swingle, Donald M., "Effects of Arrival Time Errors in Weighted Range Equation Solutions for Linear Base Sound Ranging," ASL-TR-0029, April 1979.
101. Umstead, Robert K., Ricardo Pena, and Frank V. Hansen. "KWIK: An Algorithm for Calculating Munition Expenditures for Smoke Screening/Obscuration in Tactical Situations," ASL-TR-0030, April 1979.
102. D'Arcy, Edward M., "Accuracy Validation of the Modified Nike Hercules Radar," ASL-TR-0031, May 1979.
103. Rodriguez, Ruben, "Evaluation of the Passive Remote Crosswind Sensor," ASL-TR-0032, May 1979.
104. Barber, T.L., and R. Rodgriquez, "Transit Time Lidar Measurement of Near-Surface Winds in the Atmosphere," ASL-TR-0033, May 1979.
105. Low, Richard D.H., Louis D. Duncan, and Y.Y. Roger R. Hsiao, "Microphysical and Optical Properties of California Coastal Fogs at Fort Ord," ASL-TR-0034, June 1979.
106. Rodriguez, Ruben, and William J. Vechione, "Evaluation of the Saturation Resistant Crosswind Sensor," ASL-TR-0035, July 1979.
107. Ohmstede, William D., "The Dynamics of Material Layers," ASL-TR-0036, July 1979.
108. Pinnick, R.G., S.G. Jennings, Petr Chylek, and H.J. Auvermann "Relationships between IR Extinction, Absorption, and Liquid Water Content of Fogs," ASL-TR-0037, August 1979.
109. Rodriguez, Ruben, and William J. Vechione, "Performance Evaluation of the Optical Crosswind Profiler," ASL-TR-0038, August 1979.
110. Miers, Bruce T., "Precipitation Estimation Using Satellite Data" ASL-TR-0039, September 1979.
111. Dickson, David H., and Charles M. Sonnenschein, "Helicopter Remote Wind Sensor System Description," ASL-TR-0040, September 1979.
112. Heaps, Melvin, G., and Joseph M. Heimerl, "Validation of the Dairchem Code, I: Quiet Midlatitude Conditions," ASL-TR-0041, September 1979.
113. Bonner, Robert S., and William J. Lentz, "The Visioceilometer: A Portable Cloud Height and Visibility Indicator," ASL-TR-0042, October 1979.
114. Cohn, Stephen L., "The Role of Atmospheric Sulfates in Battlefield Obscurations," ASL-TR-0043, October 1979.
115. Fawbush, E.J. et al, "Characterization of Atmospheric Conditions at the High Energy Laser System Test Facility (HELSTF), White Sands Missile Range, New Mexico, Part I, 24 March to 8 April 1977," ASL-TR-0044, November 1979
116. Barber, Ted L., "Short-Time Mass Variation in Natural Atmospheric Dust," ASL-TR-0045, November 1979
117. Low, Richard D.H., "Fog Evolution in the Visible and Infrared Spectral Regions and its Meaning in Optical Modeling," ASL-TR-0046, December 1979
118. Duncan, Louis D. et al, "The Electro-Optical Systems Atmospheric Effects Library, Volume I: Technical Documentation, ASL-TR-0047, December 1979.
119. Shirkey, R. C. et al, "Interim E-O SAEL, Volume II, Users Manual," ASL-TR-0048, December 1979.
120. Kobayashi, H.K., "Atmospheric Effects on Millimeter Radio Waves," ASL-TR-0049, January 1980.
121. Seagraves, Mary Ann and Duncan, Louis D., "An Analysis of Transmittances Measured Through Battlefield Dust Clouds," ASL-TR-0050, February, 1980.

122. Dickson, David H., and Jon E. Ottesen, "Helicopter Remote Wind Sensor Flight Test," ASL-TR-0051, February 1980.

123. Pinnick, R. G., and S. G. Jennings, "Relationship Between Radiative Properties and Mass Content of Phosphoric Acid, HC, Petroleum Oil, and Sulfuric Acid Military Smokes," ASL-TR-0052, April 1980.